January 2020

Data Analysis Of Large Angle Beamstrahlung Monitor

Samuel Doeg Izaguirre Gamez
Wayne State University

DATA ANALYSIS OF LARGE ANGLE BEAMSTRAHLUNG MONITOR

by

SAMUEL DOEG IZAGUIRRE GAMEZ

DISSERTATION

Submitted to the Graduate School

of Wayne State University,

Detroit, Michigan

in partial fulfillment of the requirements

for the degree of

DOCTOR OF PHILOSOPHY

2020

MAJOR: PHYSICS

Approved By:

Advisor	Date

ACKNOWLEDGEMENT

This project would not have been possible without the help and cooperation of many. I would like to thank the people who helped me directly and indirectly in the completion of this project work.

First and foremost, I would like to express my gratitude to our beloved director, **Dr. Giovanni B.** , for providing his kind support in various aspects.

To my family that always have been there for me no matter the distance. To my wife that supports me in every steps of my life. To God and every old and new friend that I has made on Detroit.

TABLE OF CONTENTS

LIST OF FIGURES

LIST OF TABLES

CHAPTER 1 INTRODUCTION

Experimental high energy physics is at its core the building and operation of an accelerator which produces both intense and energetic particle beams circulating in opposite directions. There are in fact two independent accelerator circulating beams in opposite directions, and they share only a small section (the Interaction Point, or IP) where beams will collide. At the point where they collide, a complex particle detector is placed to record and later study the properties of the particle-particle collisions.

The field of high energy physics has also evolved over the decades into giant international collaborations (of order 10^3 scientists on both the accelerator and detector side) building and operating over a time scale of decades. There are two important figures of merit for any accelerator. One is the beam energy, which determines how heavy the produced particle can be.

When a heavy state can not be produced, we rely on studying it via virtual effects. Fig. 1.1 shows an electroweak second order transition where a quark flavor is changed, without changing its charge (FCNC, or flavor changing neutral current). These effects, which are second order and rare (happening about once every 10^5 B decays), are a major part of the SuperKEKB/Belle II program described below. It is clear that, if these currents are to be studied, large numbers of events need to be produced. Therefore the second parameter is the luminosity L, which relates the production rate R for a given process, and its nature-given cross section σ,

$$R = L\sigma.$$

We are interested in studying ever rarer phenomena, and therefore seek to always maximize L. The luminosity integrated over time is clearly relativistically invariant, and for ultra-relativistic beams (beams that move at speeds very close to the speed of light) it can be written as

$$L = |\mathbf{v_1} - \mathbf{v_2}| f \int d\mathbf{r} dt \rho_1(\mathbf{r}, t) \rho_2(\mathbf{r}, t).$$

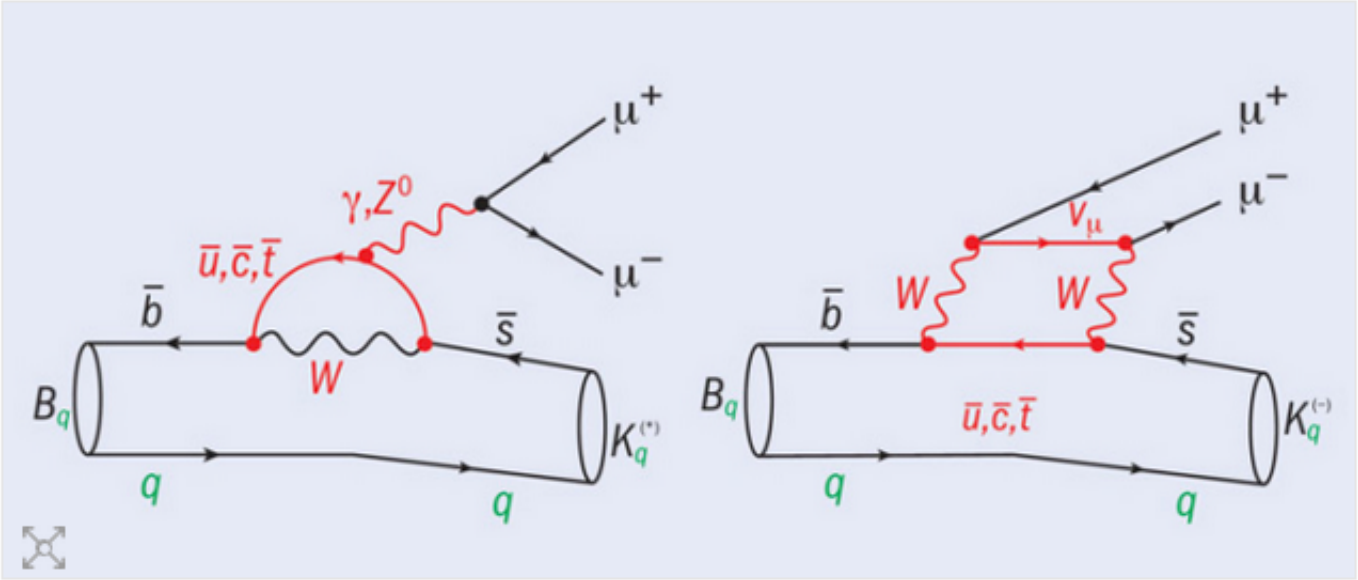

Figure 1.1: Higher order neutral current that changes the flavor of a quark.

Here $\mathbf{v_1} - \mathbf{v_2}$ is the relative velocity of the two beams, f the machine collision frequency, and $\rho_{1,2}$ are the beam density functions. When the beams are Gaussian, identical, and collinear, the integral can be easily solved to yield

$$L = f\frac{N_1 N_2}{4\pi\sigma_x\sigma_y},$$

where $N_{1.2}$ are the beam populations, and $\sigma x, y$ are the transverse beam widths. f is constrained by the maximum accelerating RF frequency, the populations are constrained by certain beam instability effects, and so the main method for controlling the luminosity is through the inverse area in the equation (sometimes called the specific luminosity).

This is achieved, at SuperKEKB as well as at other accelerators, by making the beams as small as possible in the directions transverse to the direction of motion. The SuperKEKB beams, circulating horizontally, have a projected height of order 100nm. It is very difficult to aim a 100 nm bullet, produced by accelerator 1, and hit a second, moving, 100 nm bullet produced by the independent accelerator 2. It is also difficult to make both bullets exactly equal, and when the luminosity is seen to decline, to decide which beam needs correction, which type of magnetic correction, and how much.

This is where the LABM comes into play. Using polarized beamstrahlung yields, we construct the beamstrahlung diagram, shown in Fig. 1.2. The diagram shows proper

colliding conditions (beams are transversely small and overlap), as well as conditions where the luminosity declines (one beam has moved, one beam is too big, or one beam is tilted). The pattern tells the operator (or rather an Artificial Intelligence algorithm) what type of correction is needed, and how much is needed. In an incredibly complex machine, with thousands of tunable magnets, this device reduces the corrections to a simple one, delivered right at the IP.

The value of the device is that it diagnoses the beams as they are, and at the IP where it is most important. Other devices require the operator to move the beams, which in turn changes the beams through phase space effects, or they operate away from the IP, and predictivity about IP conditions is only as good as the beam transport model in use.

In this Thesis it is discussed how the device was designed, operated, what went wrong and how we achieved our break throughs (some things went well too!).

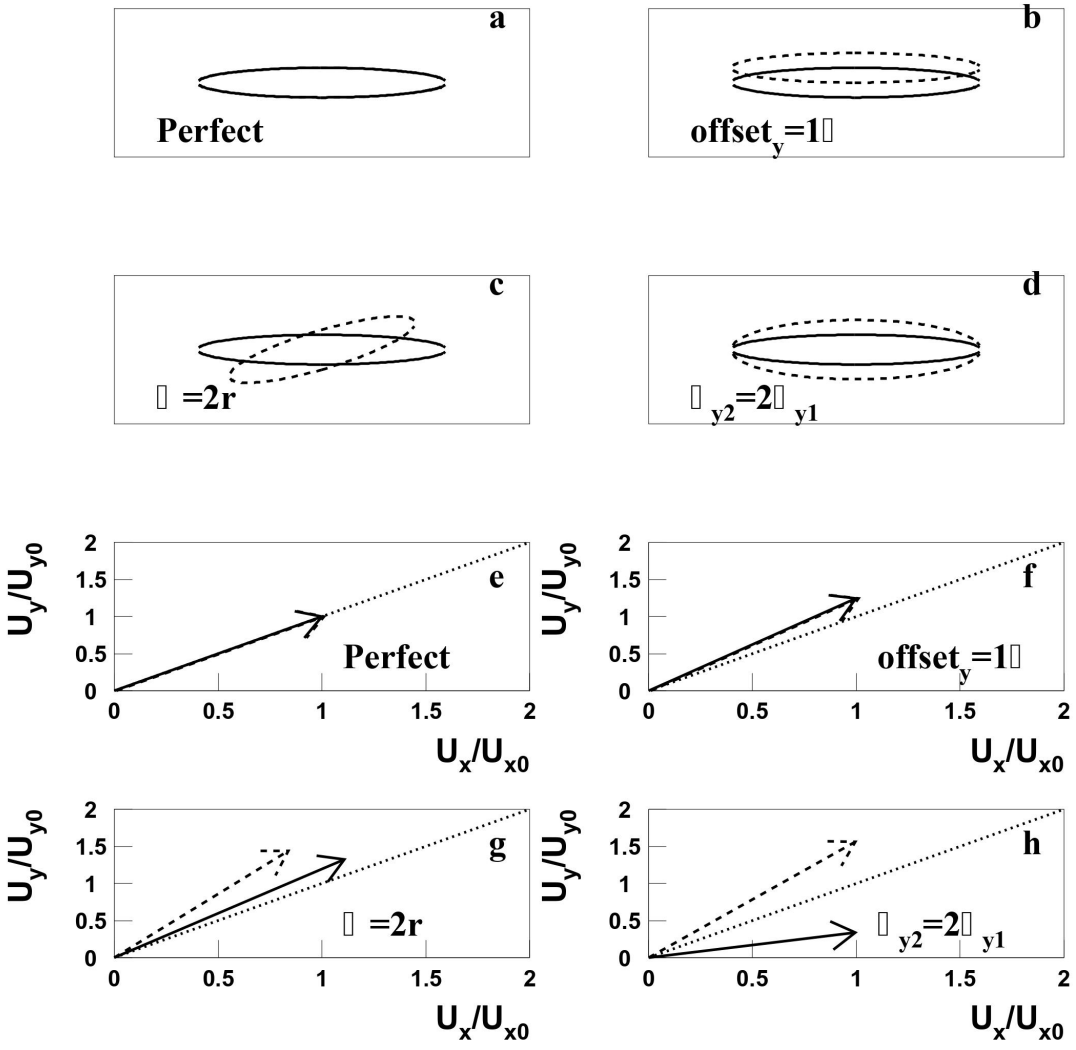

Figure 1.2: Different condition of collisions are shown in the image. a) represents a front-front perfect collision, b) a vertical offset, c) one beam is tilted, d) one of the beams is bigger than the other one.

CHAPTER 2 SUPERKEKB AND THE BELLE II EXPERIMENT

2.1 The Standard Model

Currently, we understand that the universe works under the interaction of four forces: strong, weak, electromagnetic, and gravitational. The Standard Model (SM) describes the first three using groups called unit groups. This theory was developed throughout the 1960s, starting with the quark model [1], and it was until 2012 where this model was reaffirmed with the observation of the Higgs Boson [2]. Until now, almost all experimental tests of the three forces described by the standard model they agree with their predictions, gravity is still being studied [3]. The standard model describes fundamental fields whose physical realization is particles. These represent the basis for the formation of other more complex particles. The particles of the standard model are grouped into two categories according to their spin: fermions (semi integer spin) and bosons (integer spin). This representation is shown in figure 2.1 .

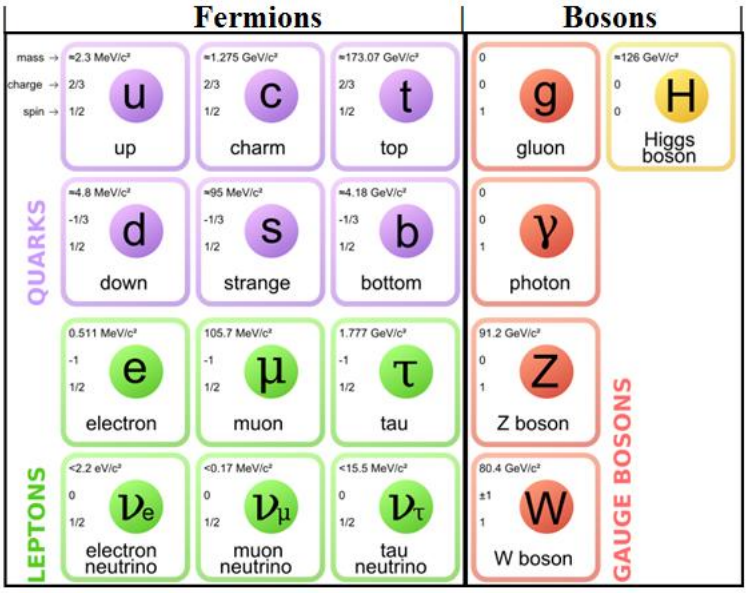

Figure 2.1: Standard model, divided into fermions and bosons and their subgroups: leptons and quarks, norm bosons and Higgs boson.

All fermions have an associated antiparticle, these particles have the same mass but differ in having the opposite electric charge. The way that the particles are arranged in the standard model image (fig 2.1) can be to better understand if you look at columns, where each column is a particle generation on the fermions side.

In the fermion family, we have two subfamilies which are quarks and leptons. The groupings of various quarks are called hadrons, of which, there are two types observed as follows: the mesons, composed of a quark and antiquark, baryons and antibaryons containing three quarks.

The first column represents the particles of the first generation these are the up quark (u), down quark (d), electron (e), and the electron neutrino (ν_e). This generation contains the lightest fermions in the standard model. In the second generation are the charm quark (c), the strange quark (s), muon (μ), and the muon neutrino (ν_μ). The fermions of this generation are a little heavier than the first-generation fermions.

In the third generation, we have the top quark (t), the bottom quark (b), tau lepton (τ), and its neutrino (ν_τ). These fermions are the heaviest of the standard model. In our fermion arrangement, we have another significant characteristic. In each row, we can see the charges of the particles are equal. That is, in the first row quarks u, c, and t have a charge of (2/3) e, where -e is the charge of the electron. In the second line, we see the quarks d, s, and b, which have a charge of (-1/3) e, and finally, we have the leptons e, μ, and τ, which have charge -e, and the neutrinos that have no charge. For the quark family, we consider another property which is the color charge which comes from strong force, this is normally labeled as red, green, and blue. The proper combination of three colors red, green, and blue or color plus anticolor is colorless and is the combination that allows us to form hadrons.

Bosons interact with leptons and quarks, in addition to interacting with themselves. These are divided into two categories: norm boson (figure 2.1, red) and the Higgs boson (fig 2.1 yellow). Norm bosons have spin integer 1 and some have no mass, such as photon and gluon, but the W and Z bosons have mass.

2.2 SUPERKEKB

A particle accelerator is made of multiple parts with different tasks, some of those tasks consist of generating, separating, and accelerating beams. Accelerators can be of two types: linear or circular. KEKB was a circular accelerator at the KEK laboratory in Tsukuba, Japan, and was upgraded starting 2010 to Super-KEKB (figure 2.3).

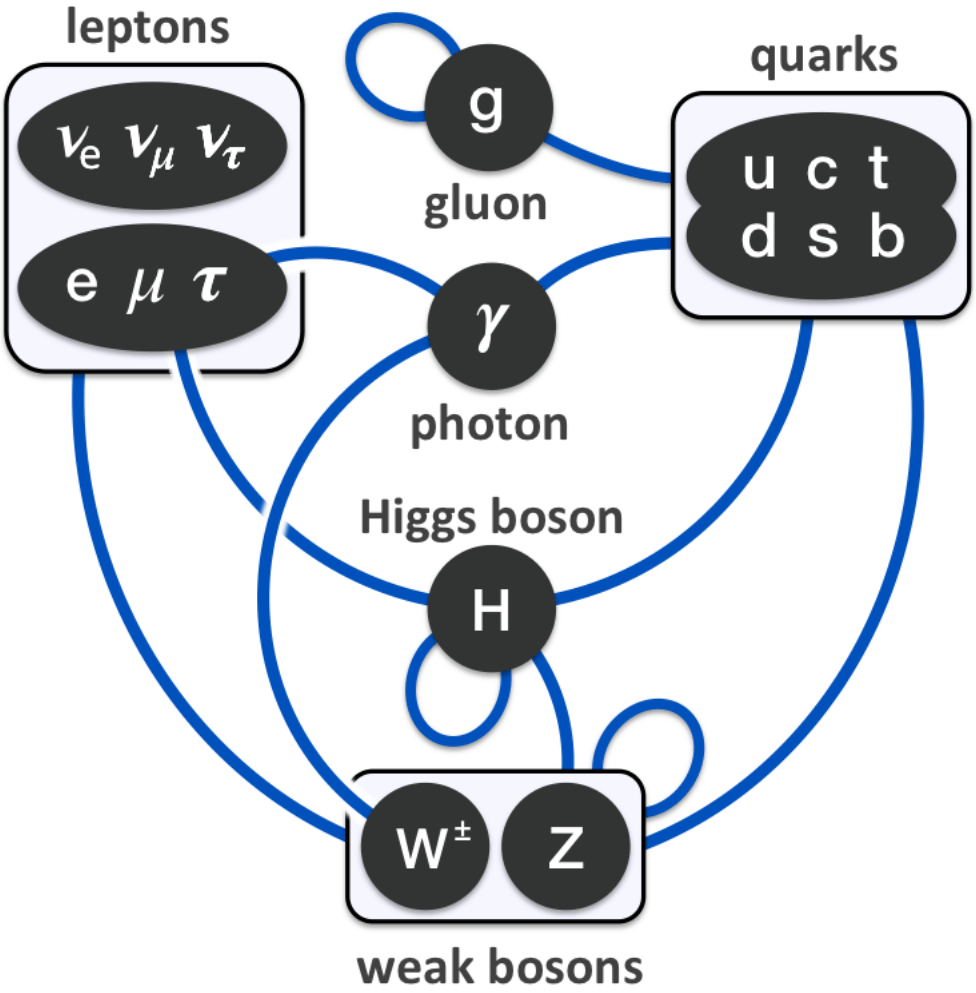

Figure 2.2: Diagram of the interaction between bosons and fermions.

KEK stands for the High Energy Accelerator Research Organization (in Japanese) . This contains a significant number of experiments, including Belle II. The collaboration of Belle II is made up of around ∼1000 researchers from over 100 different universities around the world. KEKB consists of two 3016 meter long rings, located underground with a depth of 10 meters. KEKB and SuperKEKB operate with a similar scheme, but SuperKEKB has many updates to keep the beam at nano scale [4]. Below is a schematic of SuperKEKB (figure 2.4).

The two tubes where the beams travel are placed in the same tunnel side by side, they are called beam pipes. The ring where the electrons travel is HER (High Energy Ring) and where the positrons travel is LER (Low Energy Ring). Only in one zone of SuperKEKB,

Figure 2.3: Aerial photograph of the KEK laboratory

the two tubes are joined, and the beams collide. This zone is called (Interaction Region) and around this area is the Belle II detector. KEKB and SuperKEKB produce collisions with center of mass energy corresponding to the $\Upsilon(4S)$. At that energy, the B mesons are produced almost at rest and with a good cross section of 1.3 nb.

The machine, and in particular the IP, are optimized for the study of B mesons. In the interaction region (IR) the diameter of the Beam Pipe is reduced from 20mm to 9mm and the inside of the beam pipes will be coated with a small layer of gold. This is for the purpose of absorbing as much as possible the synchrotron radiation and to protect the silicon detector, which is the closest to the interaction point [5]. KEKB and SuperKEKB beam parameters are shown in table 2.1. The separation time between one bunch to the next one is 4ns.

2.3 BELLE II

As shown in Figure 2.5, Belle II is a multi-layer detector in cylindrical shape. The Belle II detector is a general-purpose particle detector. It contains layers specialized in detecting particle decays, momenta, speeds, and energies. Starting from the center are the silicon vertex detector, PXD, the drift chamber, the particle identification detectors, the electromagnetic calorimeter, and the muon detector which is also a hadron calorimeter [5].

The silicon detectors represents the first layer of this detector and detects particles

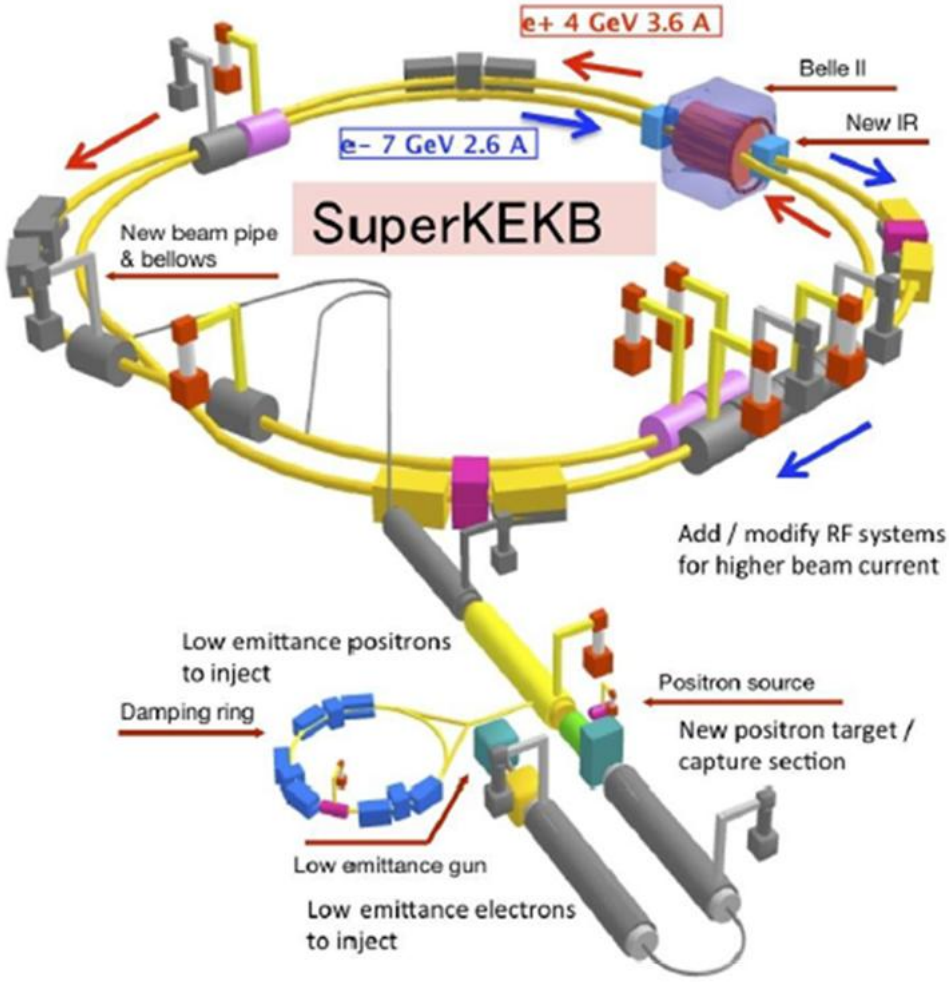

Figure 2.4: Scheme of the SuperKEKB experiment, Blue arrow show the direction of electron beam and Red arrow show the direction of the positron beam. Upgrade from Kek to SuperKEKB are highlighted.

	KEKB		SUPERKEKB	
	LER	HER	LER	HER
Energy (GeV)	3.5	8.0	4.0	7.0
Beam Current (A)	1.637	1.188	3.6	2.62
Circunference (m)	3016			
Luminosity ($cm^{-2}s^{-1}$)	2.1×10^{34}		8×10^{35}	
σ_y^* (nm)	940	940	48	63
β_y^* (mm)	5.9	5.9	0.27	0.3
σ_x^* (μm)	147	170	10	10
β_x^* (mm)	1200	1200	32	25
σ_z^* (nm)	6	7	6	5
Number of Bunches	1584		2503	

Table 2.1: Comparison table about most important parameters between KEKB and SUPERKEKB

that originate from points other than the IP (vertex detector). The next layer is the drift chamber which captures the path traveled by the charged particles to determine their momenta.

The inner layer is enclosed by the Cherenkov detectors, which are part of the system for particle identification. These detectors measure the pattern of Cherenkov light produced by particles passing through the detectors; together with the track parameters, including momentum, they allow for the identification of particles wit different masses, most importantly pions and kaons.

The Belle II Cherenkov ring layer is surrounded by an electromagnetic calorimeter which measures the energy and position of electrons and photons. Hadrons generally penetrate this layer and their energy is measured in the hadron calorimeter, where muons will also leave a unique signature that idenitfies them as muons.

The general purpose of this upgrade from Belle to Belle II is to increase the luminosity by a factor of 50, and that will allow us to search for new physics.

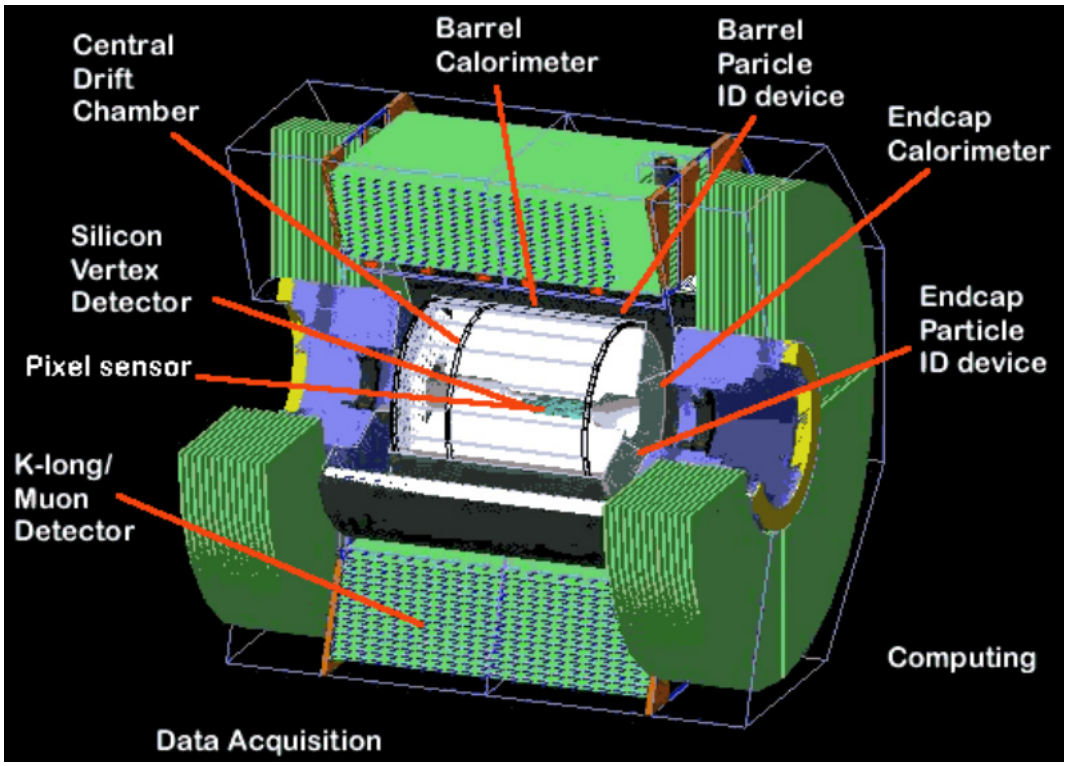

Figure 2.5: Belle II general schema

2.4 Radiation

In this Section we discuss the radiation phenomena we have to contend with when operating the LABM.

2.4.1 Synchrotron radiation

Magnetobremsstrahlung radiation or Synchrotron radiation (SR) is the electromagnetic radiation produced by moving charged particles, when they are subject to acceleration perpendicular to their velocity [6], For instance, it is generated using bending magnets (dipoles), but in our case we have to contend also with radiation from focusing magnets (quadrupoles). It generally has a continuous spectrum falling off exponentially at high frequencies.

Our device, the LABM, is sensitive only to visible radiation, which is a small fraction of the emitted SR. In the SuperKEKB environment, the typical SR energy is in the x-ray part of the spectrum. Also, SR is emitted with a typical angle $1/\gamma$ with respect to the instantaneous direction of the radiating particle, so within a cone of 0.07 mrad for electrons and 0.12 mrad for positrons.

In practice, visible SR is radiation that may come from a distance from our apparatus, it may have been reflected multiple times off the inside of the Beam Pipe, and also diffused by surface roughness. Our background fluxes depend on things which can not be properly simulated. A lot of our work depends on characterizing this background radiation using the data themselves so we can extract a signal.

2.4.2 Beamstrahlung.

There is another radiation coming from the interaction region, this is the Beamstrahlung (BM). This particular radiation exists due to the interactions between the two charged beams. The electromagnetic fields from one beam bend the second beam. BM can be used as a tool to optimize particle colliders thus increasing the luminosity [7].

The BM power has the same classical dependence on particle (mass) and bending force (magnetic field). It is proportional to $\frac{E^2}{m^4}$, where E is the beam energy and m is the mass of the particles in the beams. Consequently would be easier to detect BM in e^-e^+ collisions. There is BM in every particle collider with charged particles but only at

SuperKEKB is viable for use.

We work in a specific regime, detecting light at about 8 mrad off the beam axis. At such angles three effects appear. The first is that we can use the short magnet approximation, valid when the observation angle θ is small but still much larger than $1/\gamma$. This is good because in the limit of rigid beams (a good approximation) the yields can be computed numerically.

The second effect makes this whole project possible. At these large angles the radiation is unpolarized as a whole, when integrated over the azimuthal angle, but at specific locations (at 0, 90, 180, and 270 degrees with respect to the bending force) it is 100% polarized along the direction of the bending force. In a beam-beam collision, particles will generally be deflected both vertically (y-axis) and horizontally (x-axis), but the ratio of polarizations yields information about the balance of forces during collisions, and therefore the shape of the beaams.

The third effect is that radiation from a short magnet has a much wider angular spread than regular SR. We still have to contend with reflected and diffused radiation, but this is our major way to reduce backgrounds that would otherwise be overwhelming. This effect, too, makes our project possible. We are effectively confined to work at 90 and 270 degrees, where the SR sweep does not hit directly, above 7 mrad but not above 10 mrad (where rates would be very low).

The core characteristics of the BM, polarization and spectrum, are basically related to the beams size and relative location. These characteristics reflect a diagnostic method that can be used in a storage ring to track beam collisions [8]. This is done by using mirrors to collect the light from the accelerator and study the polarization and the spectrum of radiation emitted at the point of interaction, the experimental array for collecting BM and measuring with photo multipliers will be discussed in the next chapter.

Given the SuperKEKB parameters (Table 2.1) and the position of the vacum mirror of LABM (see table 2.2), we can calculate the expected yields[9]. The range of frequencies is the visible (400-770 THz), or 350-650 nm in wavelength, where the phototubes we use can count photons.

Mirror	Distance from IP (m)	θ_{min} (mrad)	θ_{max} (mrad
OHO DOWN	4.51	8.43	8.87
OHO UP	4.57	8.32	8.76
NIKKO DOWN	4.77	7.97	9.39
NIKKO UP	4.70	8.08	8.50

Table 2.2: Vacuum mirrors positions for beamstrahlung at SuperKEKB, distance from the interaction point.

With the previous parameters is possible to estimate the number of photons per channel, Table 2.3 shows the results of a Montecarlo simulation [9].

Mirror	Ux (10^{-18}J)	Uy (10^{-18}J)	$n_{VIS,x}(10^9$	$n_{VIS,y}(10^9)$	$dn_{VIS,x}/dt$	$dn_{VIS,y}/dt$
OHO DOWN	5.04	2.54	12.88	6.56	3.22	1.64
OHO UP	5.12	2.60	13.08	6.73	3.27	1.68
NIKKO DOWN	12.96	4.02	33.15	10.39	8.29	2.60
NIKKO UP	14.03	3.88	35.97	10.02	8.99	2.51

Table 2.3: U_x and U_y are the visible (430-770 ThZ) energies per pulse for the x and y polarizations at the vacuum mirrors. $n_{VIS,x}$ and $n_{VIS,y}$ are the corresponding number of photons. $dn_{VIS,x}/dt$ and $dn_{VIS,y}/dt$ are the photons per unit second arriving at the mirror for the x and y polarizations.

With the previous expected data from synchrotron and bm we can proceed to make scans with labm and be able to characterize synchrotron and bm. According to the previous table we would have several times more photons from bm than syncrotron, this will help us during the data taking phase.

CHAPTER 3 THE LARGE ANGLE BEAMSTRAHLUNG MONITOR

3.1 LABM Introduction

In this chapter we are going to describe the Large Angle Beamstrahlung Monitor (LABM) hardware. Our device is built by a international group of physicists, on with collaborators from Saudi Arabia, Mexico and Japan. Professor G. Bonvicini is the designer and head of the collaboration [10].

The LABM is a set of four telescopes, pointed at the IP. Given the enormous radiation backgrounds in the IR, the visible radiation which we study is taken through Optical Channels (one per telescope) to a radiation quiet area downstairs from the IR [11]. The light enters an Optics Box where it is split by a system of polarizers and gratings into 8 different beams illuminating 8 PMTs per telescope. The light contains both a signal and a background component. Collimation is provided by the (vacuum) mirror, which presents a square $2 \times 2mm^2$, and a collimator placed just prior to entering the Optics Box, 8.5 to 10 meters away. The location of the beginning of each telescope is shown in Figure 3.1.

Light coming down the Beam Pipe (BP)first hits the aforementioned vacuum mirror, located against the Beam Pipe wall. This is made of beryllium, to minimize electromagnetic showers when stray particles hit it. This mirror generates a few Watts of RF heating and is air-cooled. From there light is sent through a vacuum window to the outside. A primary mirror, remotely controllable and orientable, governs the angle of observation (where we look inside the BP).

Light is then reflected multiple times inside an Optical Channel so as to be transported downstairs (5.7 meters below the Beam Line), outside the beam tunnel and past 1.5 meters of concrete through a narrow maintenance hole. At the end of its journey light is injected into the Optics Box. At entrance it is split into two beams by a Wollaston prism. The two outgoing beams lie in the same vertical plane separated by 20 degrees. One beam carries the local horizontal polarization, and the other the local vertical polarization. Each polarized beam is reflected off a ruled grating, and a rainbow with about 15 degrees angular spread is the result. The rainbow illuminates four closely packed identical PMTs,

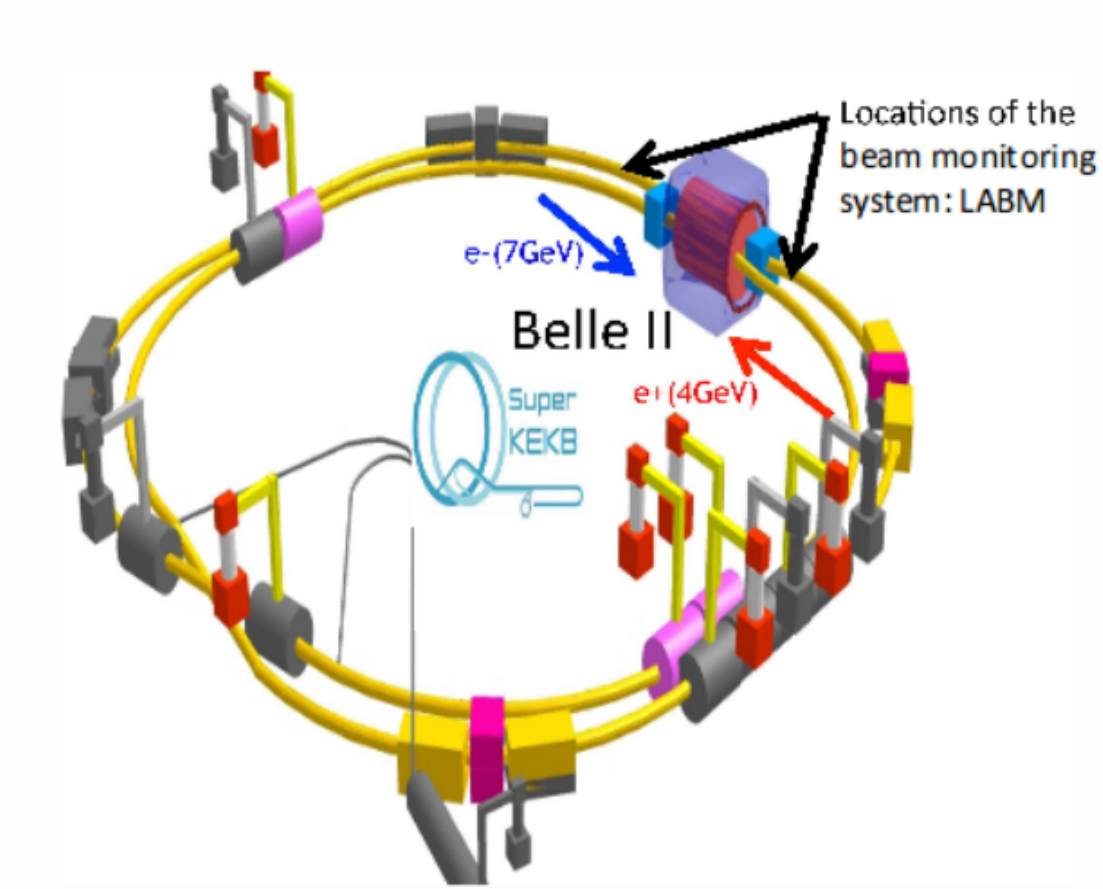

Figure 3.1: SuperKEKB, with arrows pointing at the positions of LABM primary mirrors

and it is their rates that are the active data of the LABM.

3.2 Timeline

The Large Angle Beamstrahlung Monitor "LABM" is a Beamstrahlung radiation monitor that has been installed at the SuperKEKB accelerator in the city of Tsukuba, Japan in 2015. Some series of updates have been made since 2015 due to the change of the internal scanning area inside the beam pipe. The first change was to add collimators in the optical paths in front of the optical box to reduce up to 4 times the noise in our readings. A stronger transmission gear was added to make the movement of the motors inside the primary mirrors smoother and more consistent.

In 2018 the primary elbows were modified in order to make easier the alignment, previously the primary only had 2 holes were the radiation passes though after the modification 2 large windows were added in order to have visual confirmation that the step motors were rotating properly and the flexible couplings were connected correctly (figure 3.6).

The data collection software has been updated to add the beam position reported from the accelerator group (2018). Also it has been updated to add the coordinate of the motors in the scan file (2019). A pair of larger motors and a larger primary mirror were installed in the NIKKO up channel to make it easier to see the interaction point (2019).

3.3 Hardware

There are four telescopes in LABM, 2 for electron beams (up and down) and 2 for positron beams (up and down), the channels that collects data from the electron beam are called the OHO side and the channels that collect data from positron beam are called NIKKO side. Figure 3.4.

One of the challenges is to bring the radiation from the beam pipe to the optical box avoiding the magnets that focus the beam, this is the reason why the optical path has been designed, See figure 3.3.

The only elbow with motors is the first elbow, the rest of the elbows are static but they need to be aligned before the beam starts to run otherwise would be impossible to scan the IP, we would be scanning only the sides of the beam pipe and never the

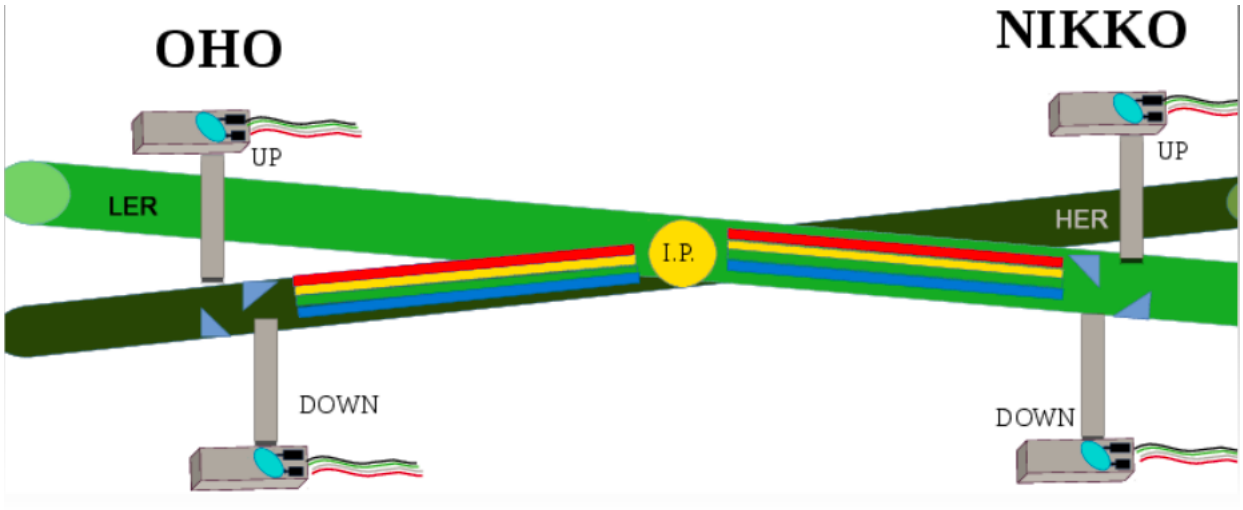

Figure 3.2: Position of the primary mirrors and vacuum mirror

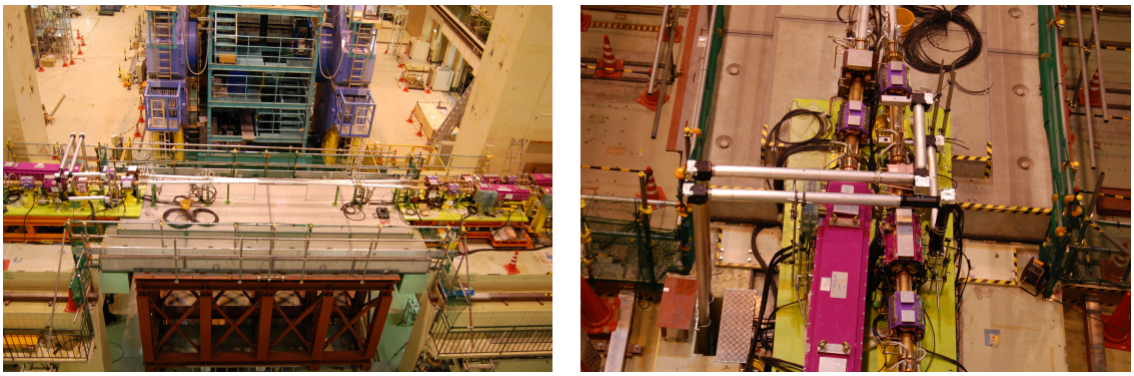

Figure 3.3: A) Aerial view of the interaction point without the Belle detector. We can see the aluminum tubes of the optical paths of LABM. Photograph of the installed LABM (left). The interaction point can be seen in the center of the image. From the interaction point to the primary mirror for each line there is a different distance, this distance is shown in table 3.1 B) Top view photograph of the LABM OHO side, it can be seen how the optical paths pass over the magnets.

Channel	Length
UP OHO	457cm
DOWN OHO	451cm
DOWN NIKKO	477cm
UP NIKKO	470cm

Table 3.1: Distance from the interaction point to the primary mirror inside beam tube for each line.

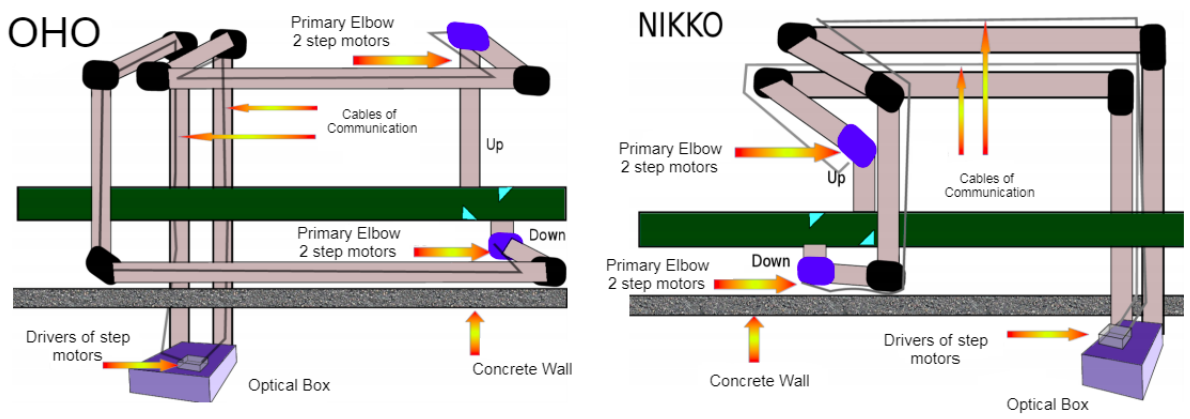

Figure 3.4: The 4 channels of LABM, oho up and oho down for electron beams, nikko up and nikko down for positron beams

interaction region. In the primary mirror we have 2 step motors (figure 3.6)connected to the flexible couplings one to one. The flexible couplings were a necessary and decisive improvement in the functionality of the primary mirrors and therefore also our ability to perform angular scans. They tolerate and adjust for small misalignments between the rotation vectors of the stepper motor and the one of the mirror.

To align the mirrors of the Optical Channels we use a laser placed vertically between the beam pipe and the primary elbow, that should hit the center of each mirror from the first elbow to the optical box. We ultimately replaced the primary pipe(figure 3.5, element 4) with a different structure (figure 3.6, element 5). The change at once eliminates any suspicion of internal reflections, while it gives us easy access for alignment (the structure is wrapped in aluminum foil before data taking).

After the last elbows that are located downstairs (figure 3.4) we have the optical box (OB), (Figure 3.7). Both OB are located in a lower radiation area than the interaction region, there is a concrete wall between the area of the optical box and the area where the primary elbows are located.

Inside the optical boxes there are 8 photo multipliers per channel, totally LABM has 32 pmt (Figure 3.8) . There is a Wollaston prism that splits the light in x and y polarizations (white arrow, Figure 3.8), then a diffraction grating is used to separate the light in spectral component. so that the LABM is able to take 32 independent measurements, we numerate the PMT as follow:

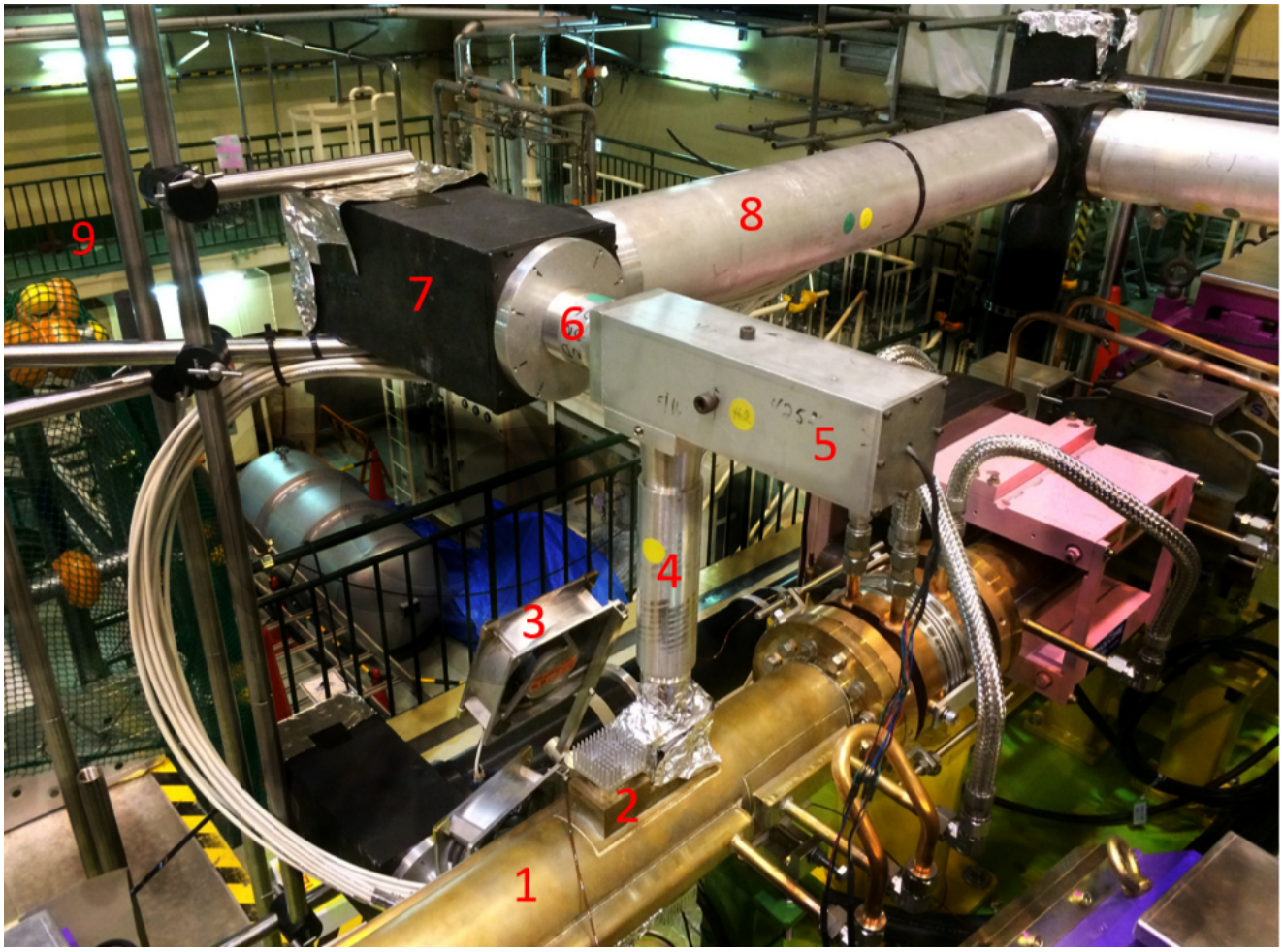

Figure 3.5: Photograph of the optical channel, 1)Beam pipe; 2)Heat sink; 3)Cooling fan; 4)Primary pipe; 5)Primary elbow; 6)Small pipe; 7)Secondary elbow; 8)Big pipe; 9)Steel rods

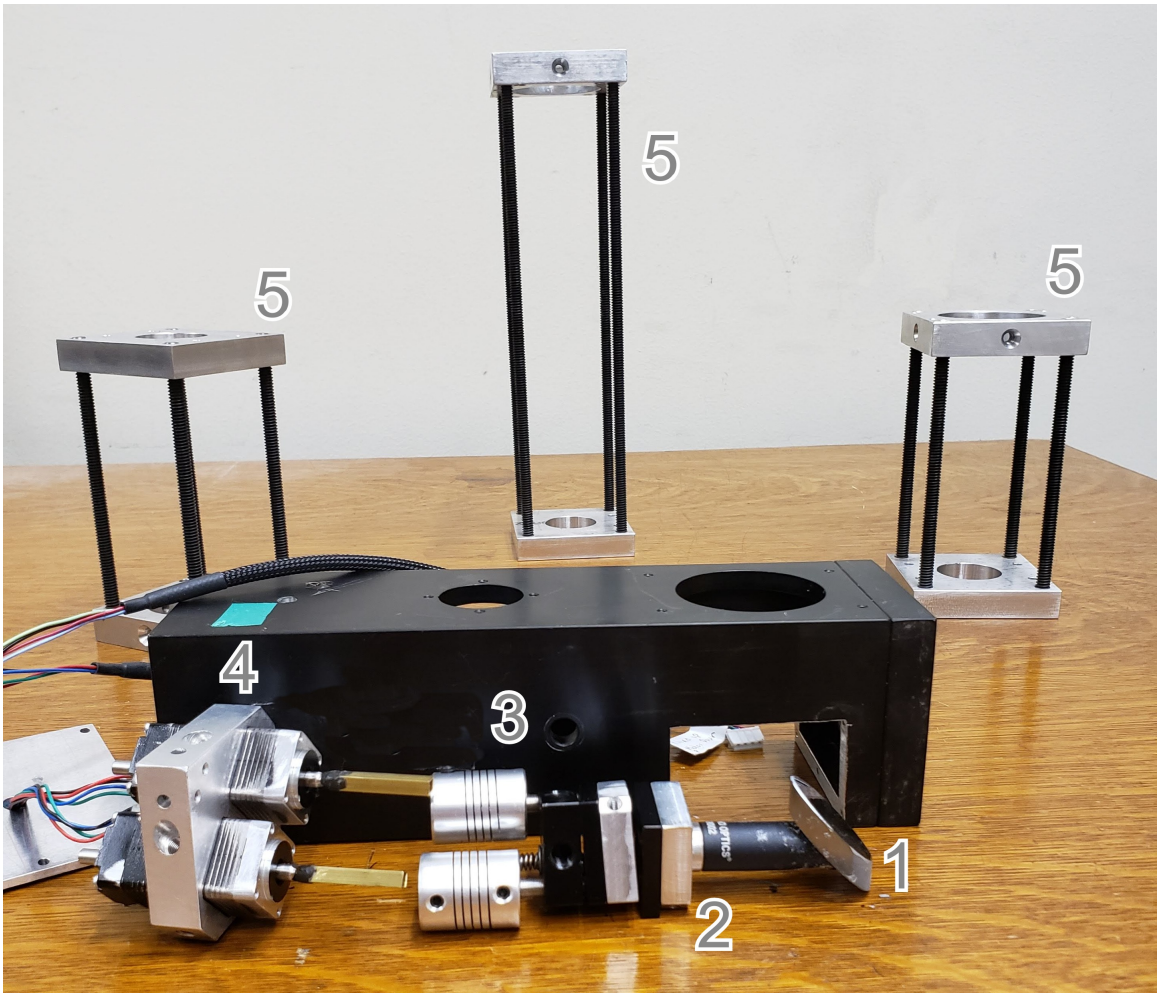

Figure 3.6: Primary mirror elements, 1) Mirror, 2) Mirror base, 3)Flexible couplings, 4)Step motors, 5) Beam pipe to primary mirror connector.

OHO UP, light Y polarized: 0 (red), 1 (green), 2 (violet), 3 (ultraviolet);
OHO UP, light X polarized: 4 (ultraviolet), 5 (violet), 6 (green), 7 (red);
OHO DOWN, light X polarized: 8 (red), 9 (green), 10 (violet), 11 (ultraviolet);
OHO DOWN, light Y polarized: 12 (ultraviolet), 13 (violet), 14 (green), 15 (red);
NIKKO UP, light X polarized: 24 (red), 25 (green), 26 (violet), 27 (ultraviolet);
NIKKO UP, light Y polarized: 28 (ultraviolet), 29 (violet), 30 (green), 31 (red);
NIKKO DOWN, light X polarized: 16 (red), 17 (green), 18 (violet), 19 (ultraviolet);
NIKKO DOWN, light Y polarized: 20 (ultraviolet), 21 (violet), 22 (green), 23 (red).

The X and Y coordinates refer to the polarization of the light in the beam pipe, the light before being counted travels inside from the interaction point to the optical box along the optical channels, and therefore the polarization changes. Each 45 degrees mirror in the channel reverses the transverse axes, resulting the following conversion.
NIKKO up (x, y) beampipe $\rightarrow$(z, y) box
NIKKO down: (x, y) beampipe $\rightarrow$ (z, y) box
OHO up: (x, y) beampipe $\rightarrow$ (y, z) box
OHO down: (x, y) beampipe $\rightarrow$ (z, y) box.

Three of four channels have even number of mirrors, and one has an odd number, and that is the reason for the discrepancy.

Once the photons hit the PMT a small electrical pulse is sent from PMT to a discriminating card (red circle, Figure 3.8), in this card pulses from the PMT that are lower than 0.010 volt are neglected and signals higher than 0.010 volt are digitized. The distance from the Optics Boxes to the LABM-computer is around of 85 meters for the NIKKO side and 25 meters for the OHO side, with 1 signal cable per PMT. In the computer room each of these cables connects to a CAEN scaler card that counts the photons and is in turn read by the LABM-computer (figure 3.9) every second. In the labm-computer there are three software programs that record all the data from LABM, these are described in the next section.

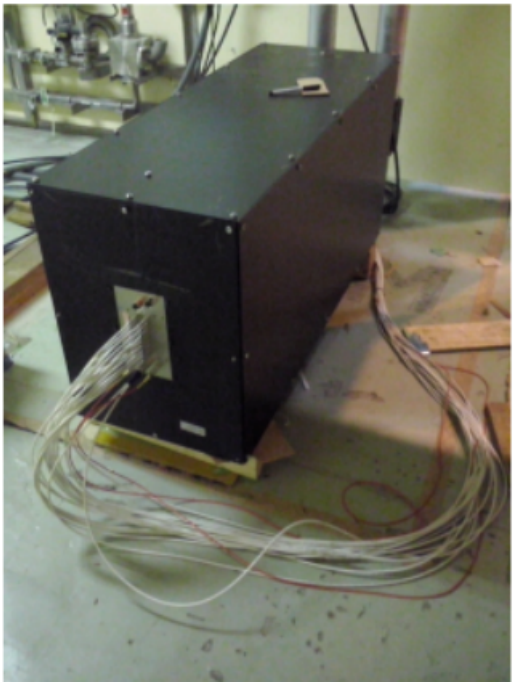


Figure 3.7: Photography of the optical box, there is an additional cover in order to verify if there is light leaking inside the optical box.

Lastly, the stepper motors in the primary elbows are controlled from the labm-computer. We control these stepper motors entirely remotely (that is, from Detroit) via VPN and ssh. Once we log in we can run the scans or move the position of the motors depending on what is needed for the data taking. The signal is sent from the labm-computer through the usb port to the driver motors located on top of the OB. There is one driver per motor, 4 drivers are on top of the OB on nikko side and another 4 on top of the OB on oho side. Finally the last connection is from the driver motor to the step motor, 1 cable per motor.

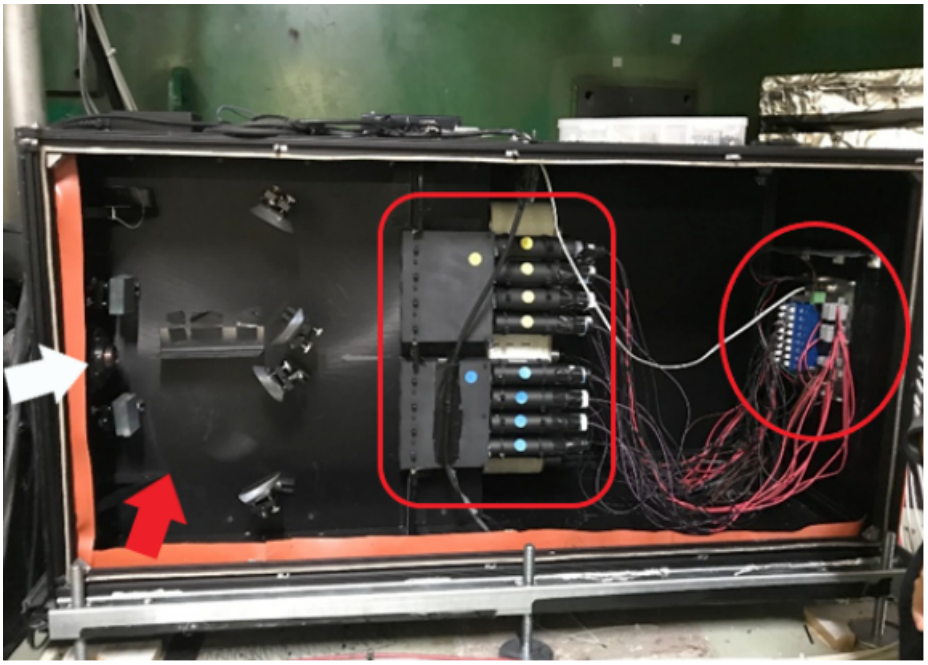

Figure 3.8: Photography of photomultipliers in the optical box, we can see the photomultipliers in the red square, in the red circle we can see the discriminator card and high voltage card for the PMT.

Figure 3.9: In this photograph we can see the card with high voltage for the PMT (1), the cables from the OB with digital signal connected to the CAEN counter card(2) and the comunication cable of optical fiber from CAEN to labm-computer (3).

3.4 Software

The motors are controlled from the LABM computer, the whole LABM system runs on c++. The software was updated in 2019 so that the route that the motors follow when being scanned in a rectangular shape was more efficient, thus cutting the scan time in half.

The typical scan that is carried out is 200,000 steps by 200,000 steps of the step motors, stopping every 5,000 or 2,000 steps as necessary. Due to the size of the region over which the scan is performed, the waiting period to finish the scan could be up to 10 hours, so it was necessary to optimize the scanning software in 2019.

The LABM computer is taking data 24 hours per day even when the beams are not running, this help us to compare the rates of the photomultipliers at different times, day and night, the one beam running or two beams running, etc. We are going to discuss 24 hours photomultipliers (PMT) graphs in the following chapters.

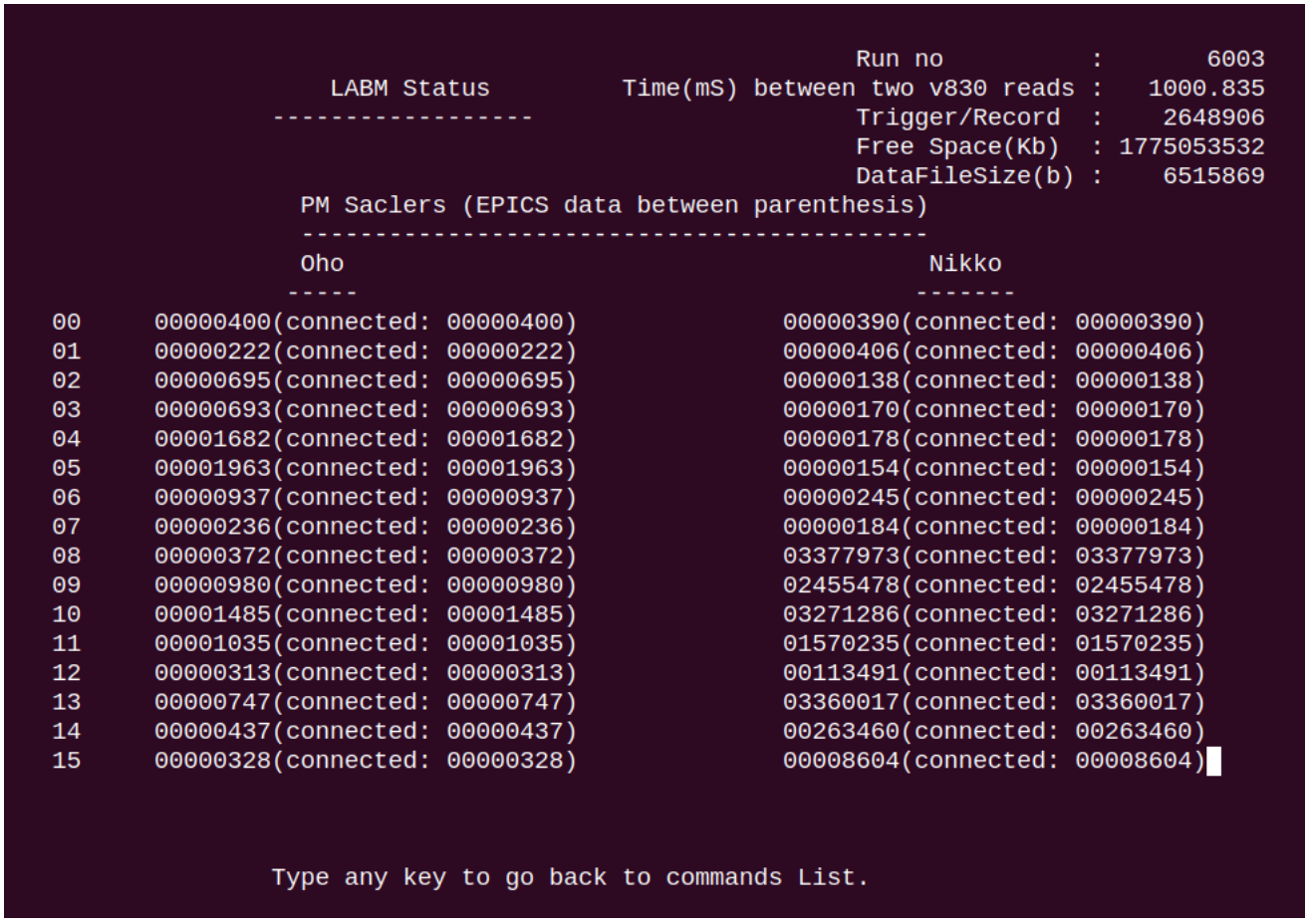

Figure 3.10: A view of LABM counter software

As we can see in Figure 3.10 we have a view of the LABM counter software, on the left side we see the 16 PMT that correspond to the OHO side, on the right side we see the values of the PMTs from nikko side. At the top there is the run number (6003), the reading time (1000ms) and the disk free space. This software helps us to verify if the OB is dark. At beam time the PMT rates should be very low. This parameters are shown as pedestal values, in chapter 4.

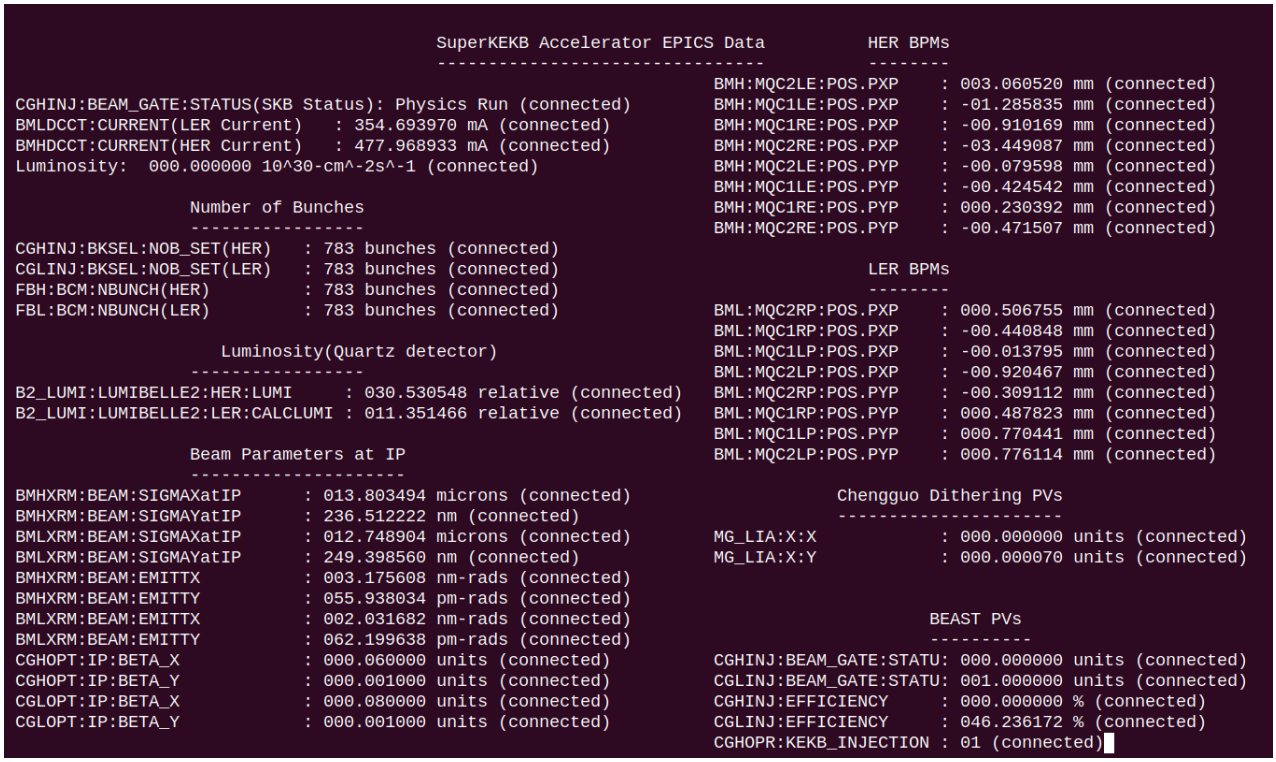

Figure 3.11: A view of LABM counter software, screen with accelerator parameters and beam positions.

Similarly there is a screen with information from the accelerator group and beam parameters, see figure 3.11.

Section 1, Beam currents and luminosity.

Section 2, Number of bunches per beam.

Section 3, Luminosity per beam.

Section 4, Beam parameters, sigma, beta.

Section 5, Electron beam position monitor.

Section 6, Positron beam position monitor.

Further, we have a program that takes the data from the PMT and makes the motors moves in order to makes a scan of the specific area needed. The first software was able only to make one scan per channel at the time. In 2019 we made an upgrade so we are now able to perform simultaneous and different scans in 4 channels.

The data is stored in text files, the maximum size is 50Mb for each file. Every file has the timestamp (Japan time zone), motor position (8 in total) , photo multiplier rates (32 in total), beam position (information from accelerator group) and miscellaneous data from the accelerator, these variables help us to clean, compare and split by specific periods during analysis.

After we upgraded the scan software we were able to perform scans in the 4 channels in parallel (figure 3.12). Basically, whereas initially we could only perform similar scans in each telescope, eventually we developed a script where each telescope had its own (wide or narrow) scan. We can choose how many of the channels we need to scan, the scan limits per motor, the number of steps per channel, the PMT rate can be store divided by the opposite beam current or just the raw rate from the PMT, how many seconds per point and the speed of the motor.

```
! Here input data to move many motors in parallel

! Steering card     Optical Line      Enabled(1: enabled or 0: disbaled)    imot1     imot2
   2DLABMSCAN            1                          1                        1         2
   2DLABMSCAN            2                          1                        3         4
   2DLABMSCAN            3                          1                        9        10
   2DLABMSCAN            4                          1                       11        12


!            Line           direction         Limit1      limit2         numberOfSteps     CurrentPos
SCANRANGE     1               1               118000      200000            41             100000
SCANRANGE     1               2                 0         200000            100            100000

SCANRANGE     2               1               118000      200000            41             100000
SCANRANGE     2               2                 0         200000            100            100000

SCANRANGE     3               1               118000      200000            41             100000
SCANRANGE     3               2                 0         200000            100            100000

SCANRANGE     4               1               118000      200000            41             100000
SCANRANGE     4               2                 0         200000            100            100000

! Rate Over Current=1  and Rate=2
 2DLABMRATE 1

! How many reads by scan point
 2DSCANREADS 2

! Motor Speed
 MOTORSPEED 1000
```

Figure 3.12: Parameters for scanning the 4 channels of LABM in parallel.

The next software is a point by point scan. With it we are able to perform scans of specific motor coordinates lists. In Figure 3.13 each section of the configuration file for the point by point scan is described. In section 1, here we can select which channels will be actively scanned. In section 2, we type the coordinate position of each motor. In section 3 (figure 3.14) we specify the file number where the new data will be stored, PEAKTIMESTAMP is the duration in seconds we will take data per point, PEAKMAXEVENTS is the number of loops.

```
!   LABM motors scans
!
! 2D scan Configuration file
! Optical Lines: We will move only primary mirrors
! 1) Oho UP: Motors 1(Oho Up Up) and 2(Oho Up Down)
! 2) Oho Down: Motors 2(Oho Down Up) and 3(Oho Down Down)
! 3) Nikko UP   : Motors  9(Nikko Up Up)    and 10(Nikko Up Down)
! 4) Nikko Down : Motors 11(Nikko Down Up)  and 12(Nikko Down Down)!

! Here input data to move many motors in parallel

! Steering card     Optical Line      Enabled(1: enabled or 0: disbaled)    imot1     imot2
   LABMLINE             1                         1                          1         2
   LABMLINE             2                         0                          3         4
   LABMLINE             3                         1                          9        10
   LABMLINE             4                         1                         11        12

!            Line           direction     Position  Direction  Position
LABMPEAKS     1              1            104200         2             106000
LABMPEAKS     1              1            104200         2             107000
LABMPEAKS     1              1            104200         2             108000
LABMPEAKS     1              1            104200         2             109000
LABMPEAKS     1              1            104200         2             110000
LABMPEAKS     1              1            104200         2             111000
LABMPEAKS     1              1            104200         2             112000
LABMPEAKS     1              1            104200         2             113000
LABMPEAKS     1              1            104200         2             114000
LABMPEAKS     1              1            104200         2             115000
LABMPEAKS     1              1            104200         2             116000
LABMPEAKS     1              1            104200         2             117000
LABMPEAKS     1              1            105000         2             106000
LABMPEAKS     1              1            105000         2             107000
LABMPEAKS     1              1            105000         2             108000
LABMPEAKS     1              1            105000         2             109000
LABMPEAKS     1              1            105000         2             110000
```

Figure 3.13: First part of the configuration file for point by point scan.

The point by point scan can be done with the four channels at same time, the file created will have a new record every second with the motor position and the rates of the PMTs. With this last block of data we can proceed to perform the analysis.

```
LABMPEAKS       4               1               96400           2               76400
LABMPEAKS       4               1               96400           2               77400
LABMPEAKS       4               1               96400           2               78400
LABMPEAKS       4               1               97400           2               75400
LABMPEAKS       4               1               97400           2               76400
LABMPEAKS       4               1               97400           2               77400
LABMPEAKS       4               1               97400           2               78400
LABMPEAKS       4               1               98400           2               75400
LABMPEAKS       4               1               98400           2               76400
LABMPEAKS       4               1               98400           2               77400
LABMPEAKS       4               1               98400           2               78400
LABMPEAKS       4               1               99400           2               75400
LABMPEAKS       4               1               99400           2               76400
LABMPEAKS       4               1               99400           2               77400
LABMPEAKS       4               1               99400           2               78400
! Peaks Data file name
PEAKSDATADISK /media/DataDisk/labm/peaks/data

! Peaks data taking run number
PEAKSRUNNUMBER 36

! time of a peak data taking in seconds
PEAKSTIMESTAMP 5

! if = 0 means run will go forever with no event limit
PEAKSMAXEVENTS   0

! TimeStamp for PVs record in seconds
PVTIMESTAMP      1

! TimeStamp for PMs record in seconds
PMTIMESTAMP      1
```

Figure 3.14: Second part of the configuration file for point by point scan.

CHAPTER 4 DATA ANALYSIS AND ANGULAR SCANS

4.1 Data flow

In the LABM computer there are 3 programs that run in parallel for data taking.

1. Photomultiplier counter. It saves in a file the timestamp and the photomultiplier rates.
2. Epics, Values from the accelerator group about the beam position along the ring
3. Scan Data, motor position and photomultipliers rate.

We split the data taking in two sections: before beam time (these are 1 or 2 weeks before the first beam runs) and running time (from when the beams starts). For example, in the first section we make sure that all the devices are working properly, the primary elbow now have a window which can be opened for inspection, and that allows us to visually verify that the step motor can move without hindrance, and also that the detector is dark.

As we can see in Figures 4.1 to 4.8 the rates when beams are absent are very stable and lower than 1000 counts per second. We usually take a long pedestal run before each SuperKEKB run. These pedestal values will be subtracted PMT by PMT during analysis (numerous pedestal values are acquired later whenever there are no beams, and pedestal values interpolated, to account for long term drift). PMTs from both sides of the detector are shown, since electrical noise is very local and in the past we have had problems with nearby noisy cables (the problem was solved by installing rubber rings between the Optical Channels and the Optics Boxes). It is clear that both sides are dark and stable.

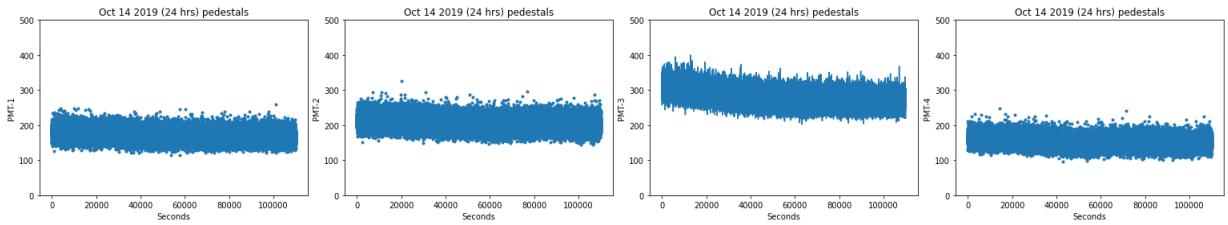

Figure 4.1: 27 hours of photo multipliers rates at no beam time, October 14 2019. X axis is the time in seconds, y axis is the rate of each photo multiplier. OHO UP channel.

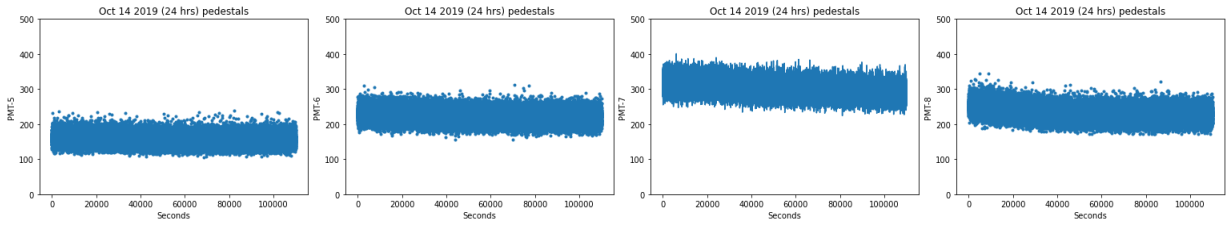

Figure 4.2: 27 hours of photo multipliers rates at no beam time, October 14 2019. X axis is the time in seconds, y axis is the rate of each photo multiplier. OHO UP channel.

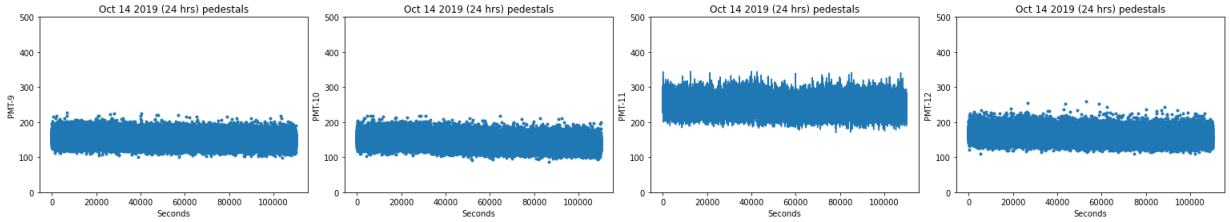

Figure 4.3: 27 hours of photo multipliers rates at no beam time, October 14 2019. X axis is the time in seconds, y axis is the rate of each photo multiplier. OHO DOWN channel.

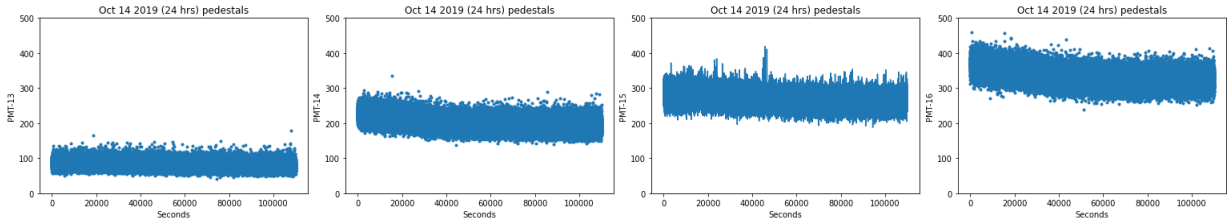

Figure 4.4: 27 hours of photo multipliers rates at no beam time, October 14 2019. X axis is the time in seconds, y axis is the rate of each photo multiplier. OHO DOWN channel.

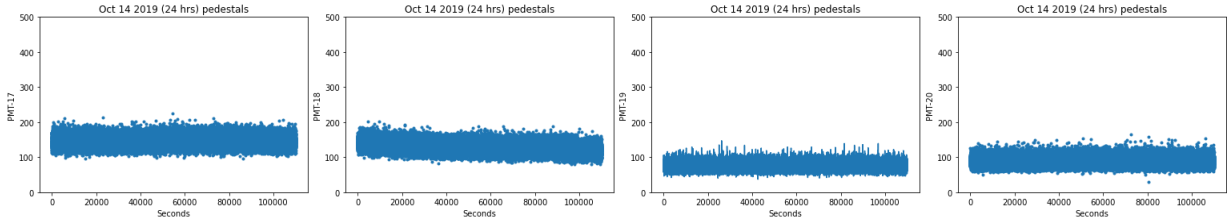

Figure 4.5: 27 hours of photo multipliers rates at no beam time, October 14 2019. X axis is the time in seconds, y axis is the rate of each photo multiplier. NIKKO UP channel.

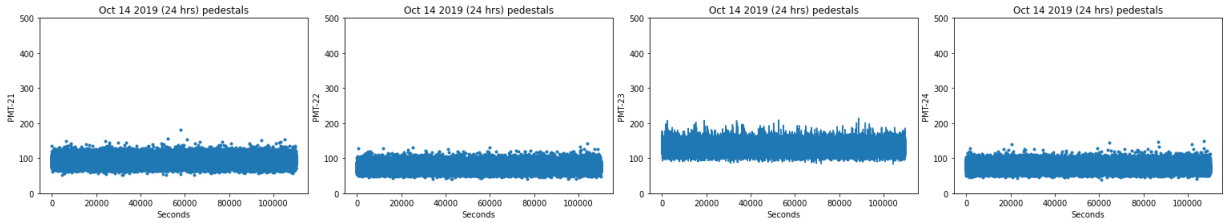

Figure 4.6: 27 hours of photo multipliers rates at no beam time, October 14 2019. X axis is the time in seconds, y axis is the rate of each photo multiplier. NIKKO UP channel.

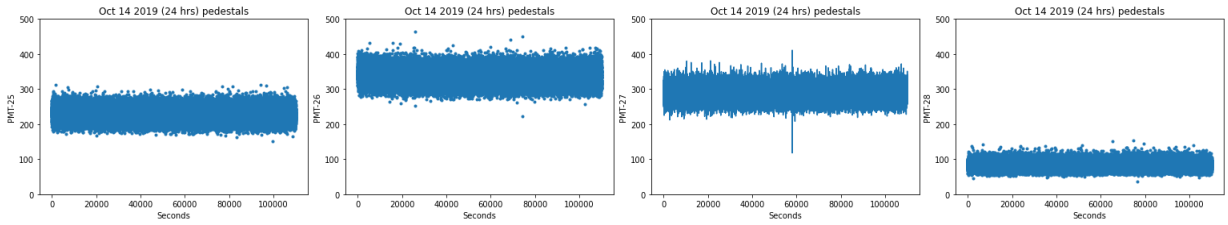

Figure 4.7: 27 hours of photo multipliers rates at no beam time, October 14 2019. X axis is the time in seconds, y axis is the rate of each photo multiplier. NIKKO DOWN channel.

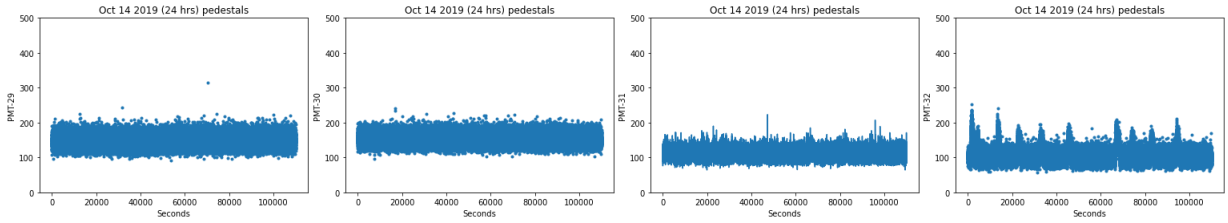

Figure 4.8: 27 hours of photo multipliers rates at no beam time, October 14 2019. X axis is the time in seconds, y axis is the rate of each photo multiplier. NIKKO DOWN channel.

When SuperKEKB starts injection, usually the electron beam is injected first for a couple of days (Figure 4.9). Single beam data taking is very useful to characterize backgrounds, because beamstrhlung is absent. Some time with single positron beams is usually also possible.

4.2 Angular scans.

An angular scan is the systematic motion of primary mirrors (through the stepper motors we control) so as to cover a rectangular grid in solid angle. At each point in the grid, the detector stops and takes data for 5 seconds. Point to point motion takes also of order 5 seconds.

Angular scans are fundamental for finding the IP. It is impossible to align our primary mirrors with any precision, due to a variety of effects. First, pieces connecting the primary mirror to the Beam Pipe rest on an uneven surface, due to some screws sticking out. Second, the primary mirror itself is glued to a well- aligned base, and differences in glue thickness do change the inclination of the mirror from the nominal 45 degrees. Finally, the extremely cramped conditions near the Beam Pipe prevent any possibility of precision work.

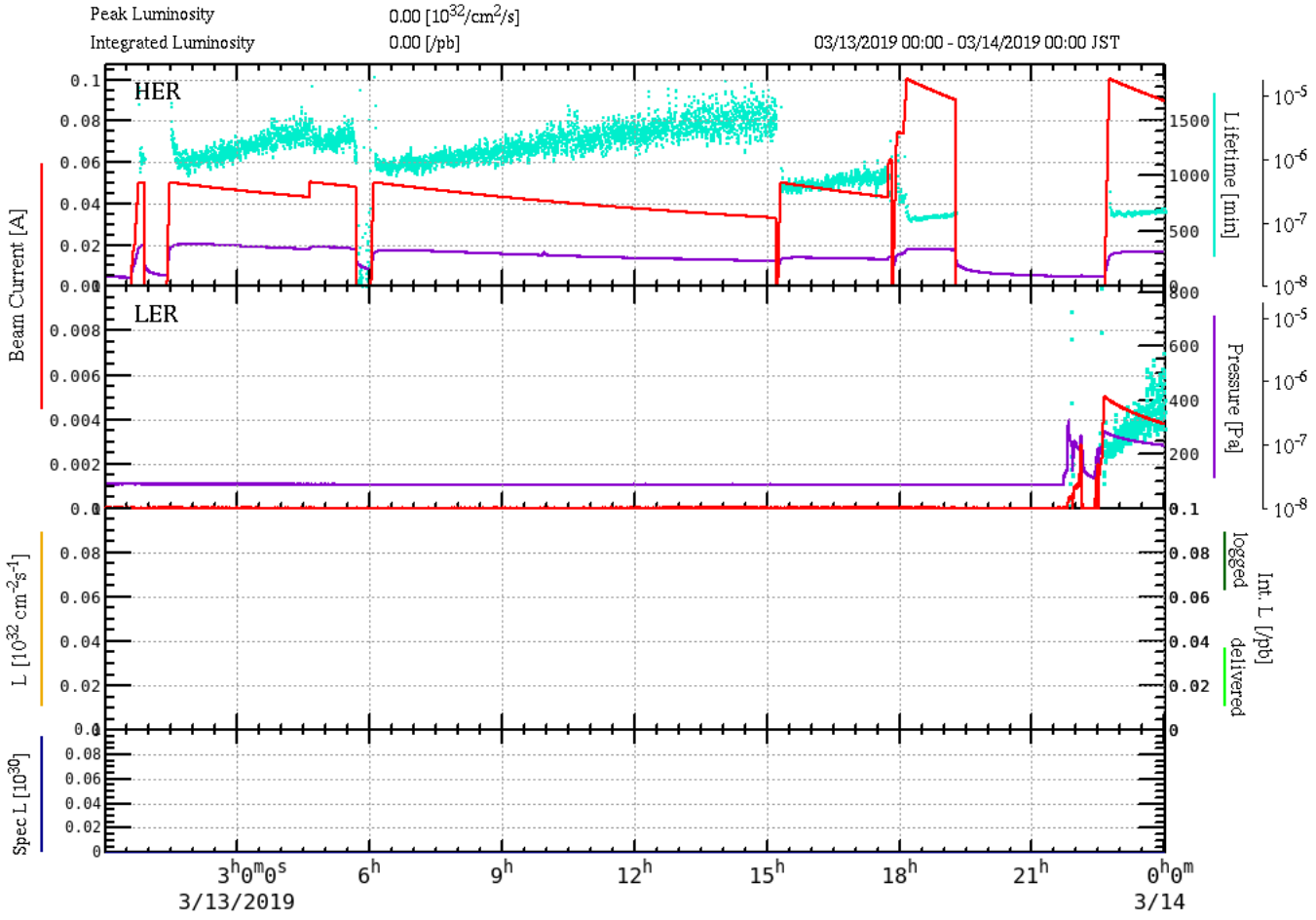

Figure 4.9: Status of high energy right and low energy ring (e- and e+) during 24 hrs.

	RATE		RATE
PMT1	175	PMT2	207
PMT3	275	PMT4	156
PMT5	160	PMT6	226
PMT7	297	PMT8	234
PMT9	154	PMT10	142
PMT11	243	PMT12	167
PMT13	83	PMT14	202
PMT15	271	PMT16	324
PMT17	153	PMT18	126
PMT19	80	PMT20	96
PMT21	98	PMT22	80
PMT23	136	PMT24	80
PMT25	241	PMT26	356
PMT27	305	PMT28	89
PMT29	156	PMT30	164
PMT31	115	PMT32	105

Table 4.1: Pedestals for every PMT.

In the past, before the narrow Beam Pipe needed for B physics was installed, sufficient detail was seen in an angular scan that the IP could be uniquely identified. For example see the NIKKO DOWN scan performed in 2016 with the wide Beam Pipe, fig. 4.10. Because the last bending magnet is visible, from the IR geometry we can identify the IP. The numerous reflections off the Beam Pipe walls provide further cross checks that the pattern seen is the one expected.

Once the Beam Pipe was replaced with a narrower beam pipe, auxiliary patterns became unavailable. The figure of the Beam Pipe vertical profile, Fig. 4.11 shows that light can squeeze through a lentil shaped region very close in angle to the IP. The IP will be slightly off center with respect to it, and a long reflection streak from the inside of the inner Beam Pipe is also possible.

We started with wide scans, and as peaks of radiation were detected, we narrowed the scan to the region around the peak. Below are heat maps of the angular scans with only the electron beam at around 48mA. The limits are 50,000 to 150,000 steps of the motor 1 and motor 2, the distance between two points of data taken were 5,000 steps. (figure 4.12 and 4.13).

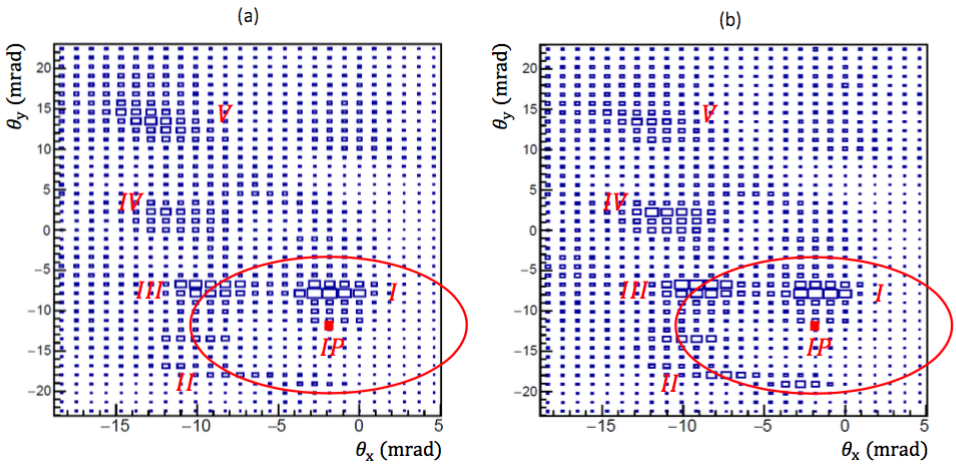

Figure 4.10: 2016 angular scan of NIKKO DOWN with red PMTs. First plot: x-polarization. Second plot: y-polarization. The IP is marked as a red square, the structures marked II-V are expected reflections. The Beam Pipe waist at the IP is also shown as a red ellipse.

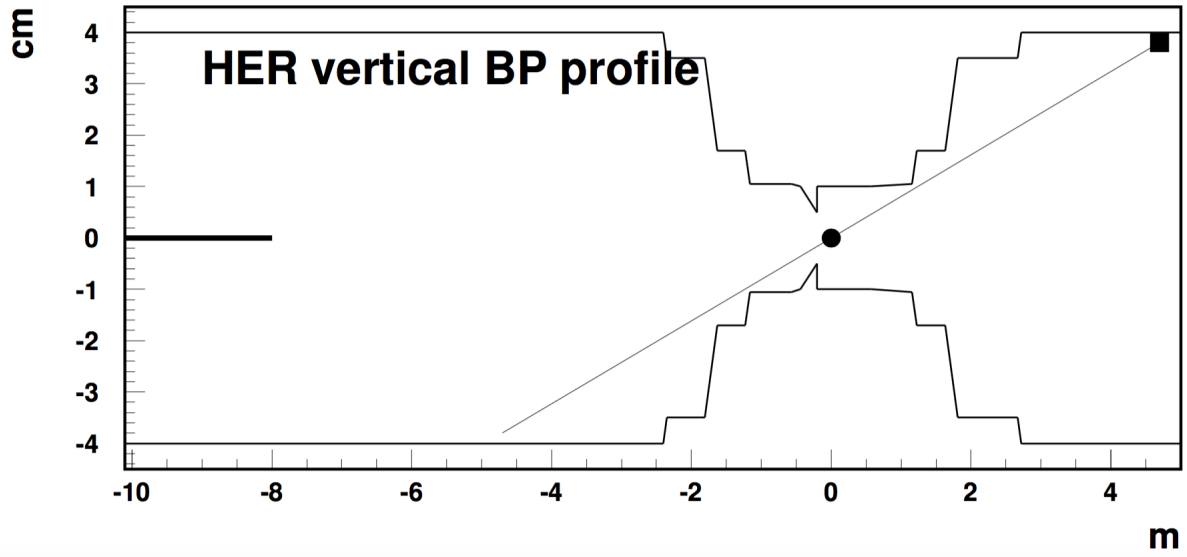

Figure 4.11: Beam pipe vertical profile, HER side. There is different scale on the axis.

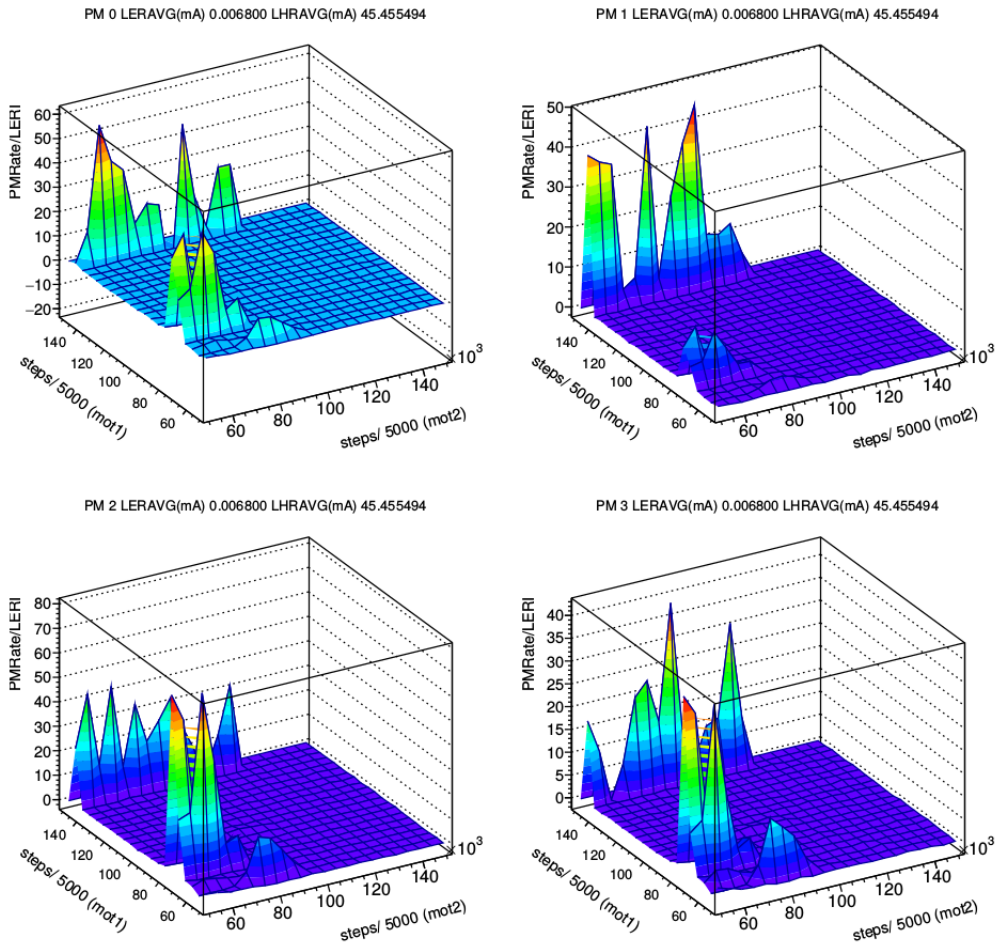

Figure 4.12: Angular Scan, OHO UP channel, March 13 of 2019, PMT 0 to 3. The z axis is the rate of the PMT divided by the HER current.

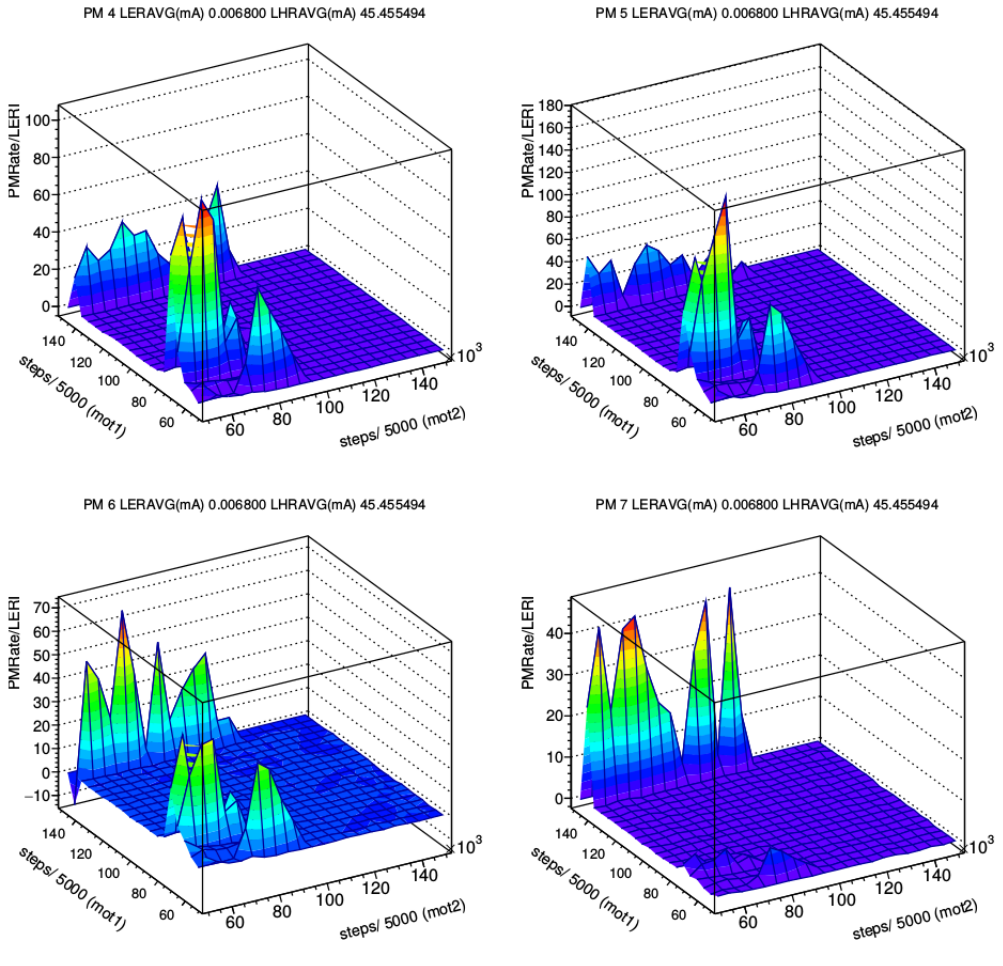

Figure 4.13: Angular Scan, OHO UP channel, March 13 of 2019, PMT 4 to 7

In the narrow scan that follows instead of having a range from 50,000 to 150,000 we go to a range of 50,000 to 80,000 (figure 4.14 and fig 4.15). A great advantage of smaller scans is that they are finished more quickly. If the beam becomes unstable during long scans, the scan stops automatically and waits for good beams to resume. Sometimes that takes days.

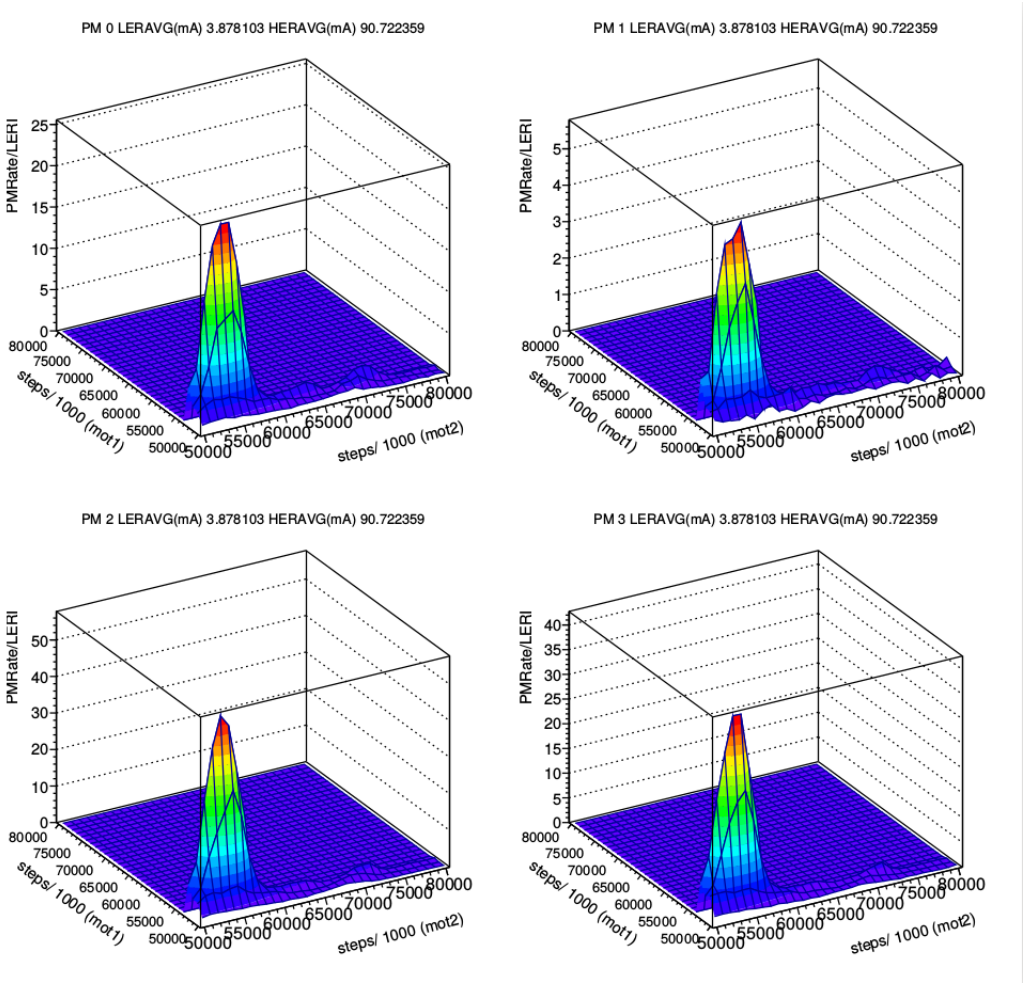

Figure 4.14: Angular scan, oho up channel, March 13 of 2019, only the electron beam is running. PMT 0 to 3.

Fig 4.14 and fig 4.15 provide a useful contrast since the difference betwween single beam and double beam data taking should be beamstrahlung. In practice mostly shape changes of the peak regions help us get oriented, since the reflection tails tend to change a lot over time.

As we can see in Figure 4.16 and Figure 4.17 the maximum rates of the PMTs are now larger than in Figure 4.14 and Figure 4.15, this is due to the presence of beamstrahlung.

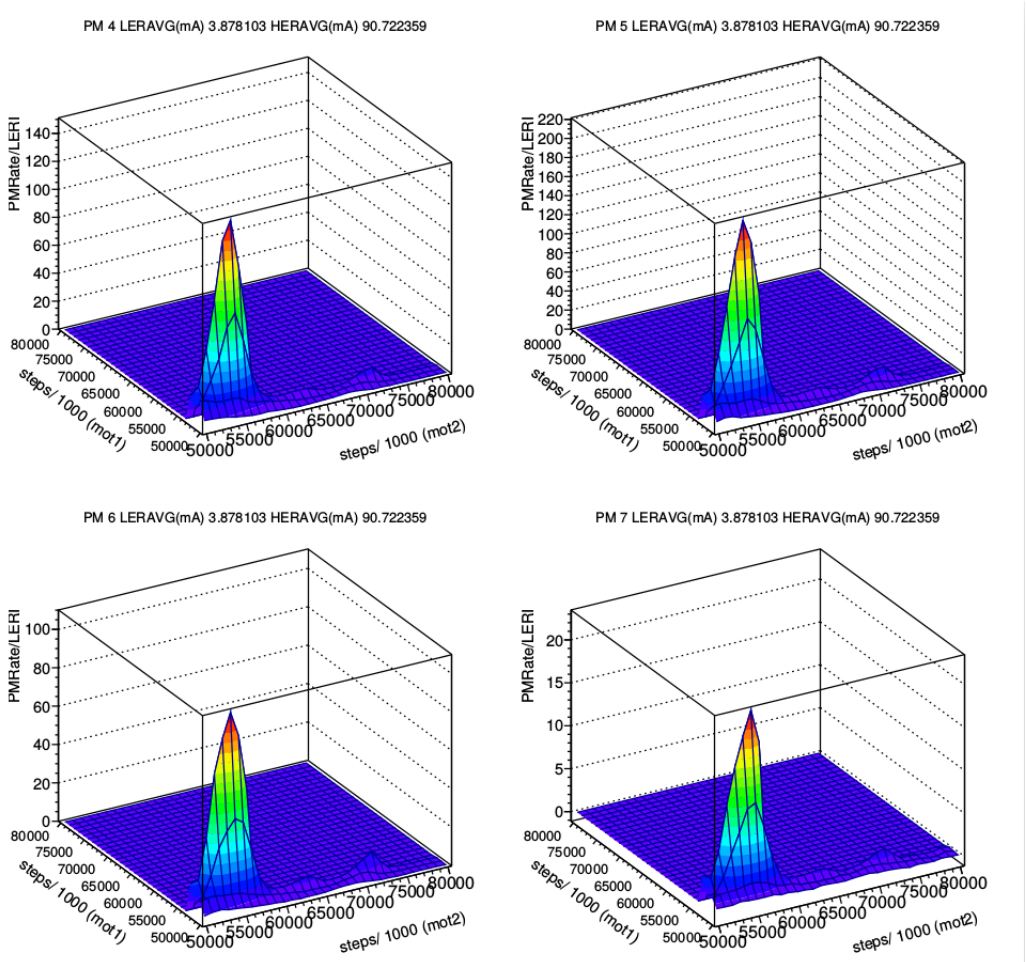

Figure 4.15: Angular scan, oho up channel, March 13 of 2019, only the electron beam is running. PMT 4 to 7.

In order to study the beamstrahlung with more detail is needed to make a very small scan point by point around the area of interest. We select by hand the motor coordinates for each channel for the point by point scan.

Having seen clear radiation peaks in our angular scans, we apply the methods described in the next Chapter to extract first evidence for large angle beamstrahlung at SuperKEKB.

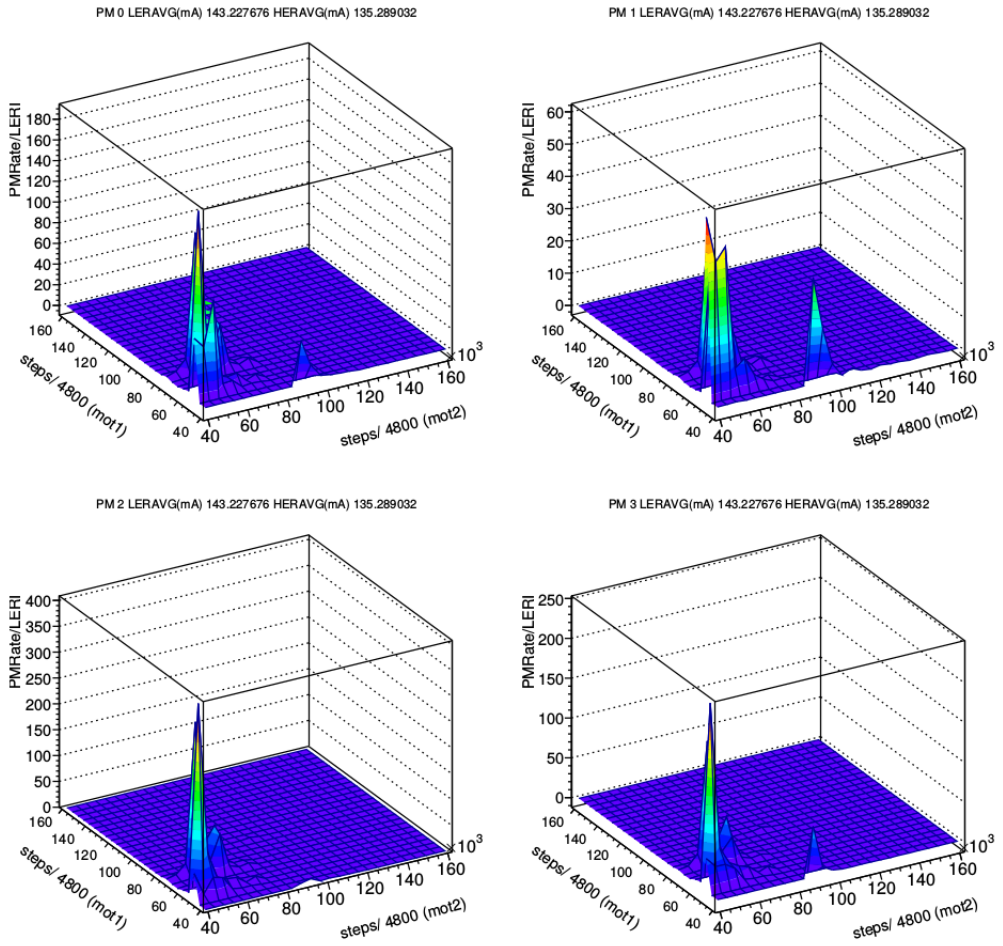

Figure 4.16: Angular scan, OHO, with both beams running, March 25 of 2019. Step size of the scan is 4800 per motor. PMT 0 to 3.

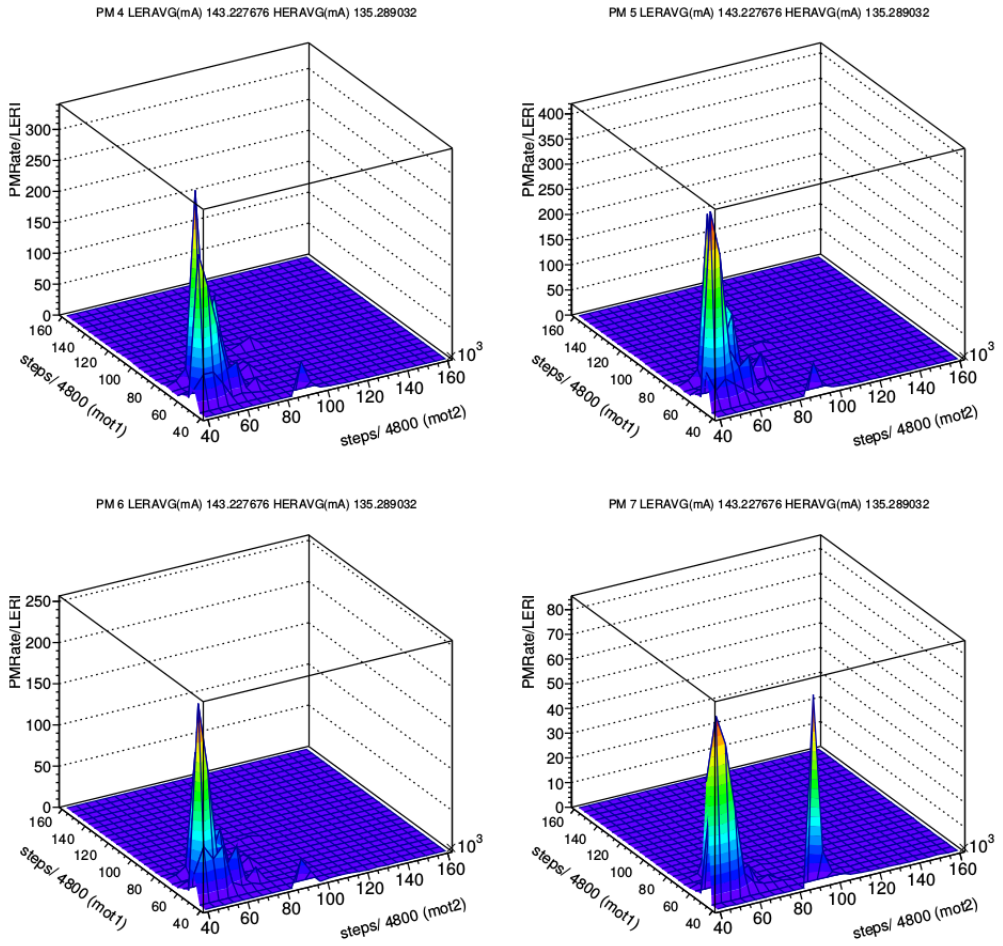

Figure 4.17: Angular scan, OHO UP, both beams running, March 25 of 2019. Step size of the scan is 4800 per motor. PMT 4 to 7.

CHAPTER 5 EXPERIMENTAL RESULTS

Having identified the most likely locations for the IP, we turn our attention to establishing a signal. At this point in time the signal to background ratio (S/B) is fairly low. We will see below that while backgrounds scale linearly with bunch population, the signal scales as the third power. Thus our S/B will increase as the SuperKEKB machine produces more intense beams.

Having a bright spot by itself does not mean much. Figure 4.11 showed the vertical profile of the electron BP. It is clear that, together with the IP, we catch with our telescopes also quite a bit of the BP reflecting SR, also producing a bright spot. The signal spot is slightly offset (by a fraction of a mrad) with respect to the background spot. Further, we have known since 2017 that the background tends to be much more x-polarized than the signal, so that the initial signal is best seen using y-polarized light, or more accurately, that the y-polarized PMTs will show less noise. Also, red PMTs will have a better S/B because longer wavelengths are less scattered by BP roughness.

Only data from 3 telescopes are presented. OHO DOWN could not be processed in time. Nikko Up shows a clear but noisy signal, due to having run without a collimator during the latest data taking. The collimator is now installed and it is expected that the backgrounds will decrease by up to a factor of 5.5.

5.1 Properties of signal.

The quantities of interest are the total radiated power W_1 (by beam 1) and the large angle spectral distributions, $d^2W_1/d\omega d\Omega$. The formulae are [12] ,

$$W_1 = \frac{f}{c}\int dx_1 dy_1 dz_1 dT \rho_1(x_1, y_1, Z_1) P(x_1, y_1, Z_1, T), \tag{5.1}$$

where f is the beam collision frequency, and P the power emitted at any point in space and time,

$$P(x_1, y, z_1, T) = \frac{q^2}{6\pi\epsilon_0 m^2 c^3}\gamma^2 F^2(x_1, y, z_1, T). \tag{5.2}$$

The z, x variables have subscript 1 because the coordinate systems of beams 1 and 2 share the same y-axis (vertical), but the two other axes are rotated by 180 degrees minus

the crossing angle. The integrals can be separated into the $x-$ and $y-$ components of the force

$$W_{x1} = \frac{fq^4\gamma^2}{6\pi\epsilon_0 m^2c^3}\int dxdydzdt\rho_1(x,y,z,t)F_{x2}^2(x,y,z,t), \quad (5.3)$$

$$W_{y1} = \frac{fq^4\gamma^2}{6\pi\epsilon_0 m^2c^3}\int dxdydzdt\rho_1(x,y,z,t)F_{y2}^2(x,y,z,t). \quad (5.4)$$

The angular spectral distribution can be obtained from the "short magnet" approximation [8], convoluted with the beam density

$$\frac{d^2W_{i1}}{d\omega d\Omega} = \frac{fr_e\gamma^2}{\pi mc^3}a_i(\theta,\phi)\int dx_1dydz_1\rho(x_1,y,Z_1)|\tilde{F}_i(x_1,y,z_1)|^2, \quad (5.5)$$

where

$$\tilde{F}_i = \frac{1}{\sqrt{2\pi}}\int F_i(z_1)e^{-ikz_1}dz_1, \quad k = \frac{\omega(1+\gamma^2\theta^2)}{2c\gamma^2} \quad (5.6)$$

and

$$a_\sigma = \frac{(1-\gamma^2\theta^2\cos 2\phi)^2}{(1+\gamma^2\theta^2)^4}, \quad a_\pi = \frac{(\gamma^2\theta^2\sin 2\phi)^2}{(1+\gamma^2\theta^2)^4} \quad (5.7)$$

are the polarization components respectively parallel and perpendicular to the bending force.

We have a program that calculates numerically these rates, however it is instructive to derive the dependence on commonly available Epics quantities. These are the current intensities and number of bunches, both of which will vary a lot over the course of 3 months. The assumptions underlying this calculation are discussed below.

5.2 Data analysis method.

The current can be written as

$$I = NBef_0,$$

where N is the bunch population, e the elementary charge, B the number of bunches, and f_0 is the basic synchrotron frequency

$$f_0 = 3016/c.$$

(Recall that 3016m is the ring circumference). The force in Eqs. (5.3-5.4) are the forces produced by a Gaussian beam, while ρ_1 integrates to be proportional to N_1

$$F \propto N_2,\ \rho_1 \propto N_1.$$

Finally, the SR from beam 1 is proportional to N_1.

We now wish to characterize a general observation of a mixture of signal and background as a function of the Epics variables.

$$Rate_1(I, B) = \beta I_1 + \sigma \frac{I_1 I_2^2}{B^2}.$$

In deriving this equation we have absorbed e, f_0, which are unchanging, in the constant quantities. These are the background parameter β and the signal parameter σ. Dividing by I_1 we obtain

$$Norm_1(I_2, B) = \beta + \sigma \frac{I_2^2}{B^2}. \tag{5.8}$$

It is this formula that guides our analysis. The normalized rate $Norm$ has a flat component and a quadratic component. Detection of a non-zero quadratic component is tantamount to finding large angle beamstrahlung.

The formula is valid whenever beams do not change size over long periods of time. This can not be an exact approximation because the data shown here were collected during the entire month of April 2020. Sources of systematics include slight changes to the beam orbit (resulting in small changes to the background) and physical changes to the beam size, which affect in particular the y-polarized signal yields.

We also check that our signal should correspond, in an angular scan, to the image of a point through a two-collimator telescope, which is approximately a narrow trapezoid. We note below that the OHO UP signal easily satisfies such a requirement.

5.3 Data analysis to find the IP.

In the absence of a known IP, we resorted to continuous scanning. Fig. 5.1 shows the lattice for OHO UP, a 7×12 matrix. Recall that the luminous spot will generally be a combination of signal and background. The signal is a point-like source, whereas the background has a lentil shape. Once the IP is found, we will continuously scan only 3

points, the signal spot and the two spots immediately adjacent horizontally. Continuously checking those spots will assure a continuous monitoring of backgrounds.

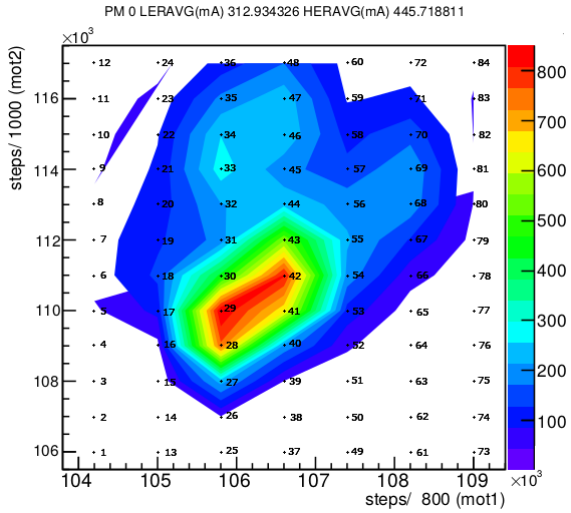

Figure 5.1: Wide scan points, OHO UP telescope. The z axis is the rate of the PMT divided by the HER current.

However, for the month of April 2020 we scanned a wide angular area, seeking to validate our procedure by observing as many spots as possible which had pure backgrounds ($\sigma = 0$). Also, currents do not vary appreciably for long periods of time (often weeks), so that the amount of data taking is justified also by the need to take data of sufficiently varying currents.

Once data are accumulated, a point by point linear fit is performed for each point of the scan. We then plot the dependence of σ on the lattice position. We choose both red PMTs for display, Figs. 5.2 and 5.3 show the σ dependence on the scan position. Peaks are seen every 12 spots, with the biggest one at position 29 for both polarizations.

Translating it into a signal rate yields a red rate of about 7.5 KHz and a total visible rate of 15 kHz, consistent with expectation, since currently beams are wider and currents lower than nominal conditions (where a total signal of 2Mhz is expected).

The presence of multiple peaks is noted. This is easily explained as follows. For OHO UP we expect a beamstrahlung spot size at the Optics Box of about 6.3 mm. This corresponds to an angular diameter of 0.6 mrad for the beamstrahlung spot. The motor angular step size in the y-direction in Fig. 5.1 is half that of the motor in the x-direction, and corresponds to approximately 0.35 mrad. With a step size less than the width of the

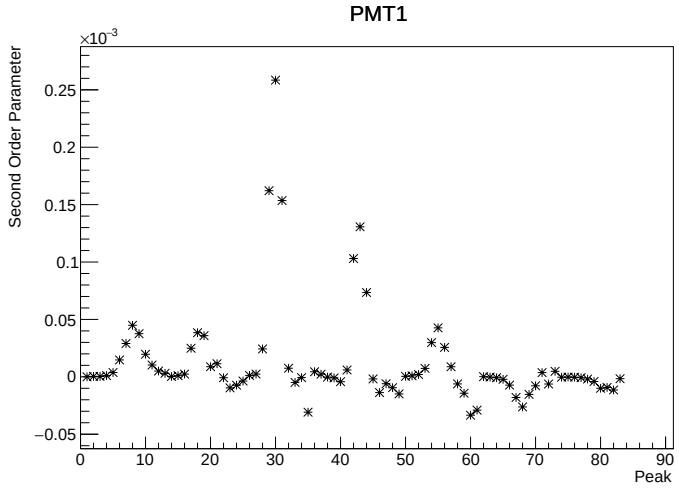

Figure 5.2: OHO UP telescope distribution of σ parameters for red y-polarized PMT.

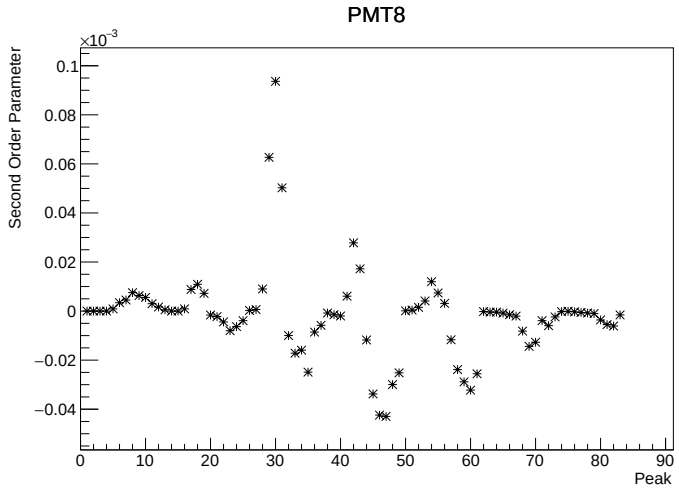

Figure 5.3: OHO UP telescope distribution of σ parameters for red x-polarized PMT.

signal beam it is normal to see the signal at more than one point.

Further, recall from. Fig. 4.11 that our signal brushes against a Beam Pipe edge. Diffraction peaks can be formed there, which can be disentangled by spectral analysis. We maintain however that the strongest peaks always correspond to the physical mirror.

OHO UP represents what we are aiming at. The IP is clearly seen, we plan to make a finer scan next time around location 29, expecting a tetrahedron-shaped distribution for σ which we can already see. We will then place our device at the vertex of the tetrahedron, and occasionally move to the left and right of the vertex (if the vertex were exactly at point 29, we would scan points 26 and 32) to monitor backgrounds. The pointing work for this telescope would then be over, and once the machine approaches nominal conditions, if the S/B is high enough, we will stop scanning altogether.

Currently OHO UP has a S/B of order 1. OHO has always had worse backgrounds than NIKKO, because the last magnets before the IP are farther back, and also because the HER BP is brushed aluminum, which scatters radiation much more than the LER pipe, which has been coated with TiN, and is much smoother.

5.4 NIKKO telescopes.

Both NIKKO telescopes were without collimators during the Spring 2020 run. In our double-collimator scheme, the first collimator is always the primary mirror, 2 mm in size. The second is a standard collimator just before the Optics Box, a square collimator 8 mm in size. With beamstrahlung spots at the Optics Boxes ranging from 6.2 to 6.9 mm, 8mm represents a satisfactory compromise (effectively, we give ourselves an extra mm to play with).

If the 8mm collimator is not present, the collimator is effectively the Wollaston prism, which is square and 19 mm in size. We did not place the collimators because we had no evidence that the telescopes had worked in the prior run. The collimator effectively restricts the field of view of the LABM and needs to be placed only after features are seen. An undergraduate collaborating with us did place collimators into these telescopes during the summer shut down, and at least for NIKKO UP we expect similar results to OHO UP in the coming Fall run.

The angular matrices for NIKKO UP and NIKKO DOWN are shown in Figs. 5.4 and 5.5 respectively.

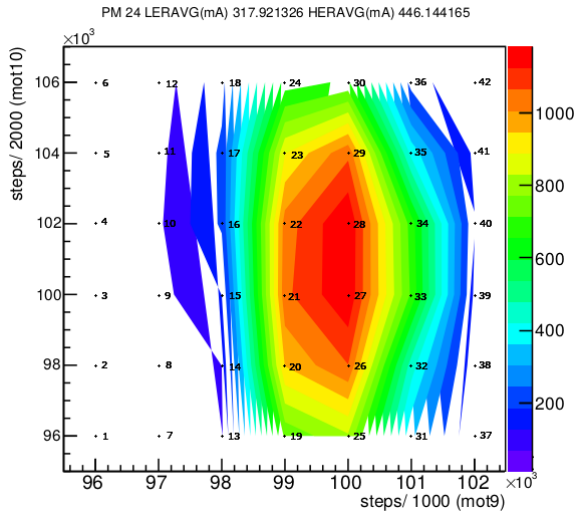

Figure 5.4: Wide scan points, NIKKO UP telescope.

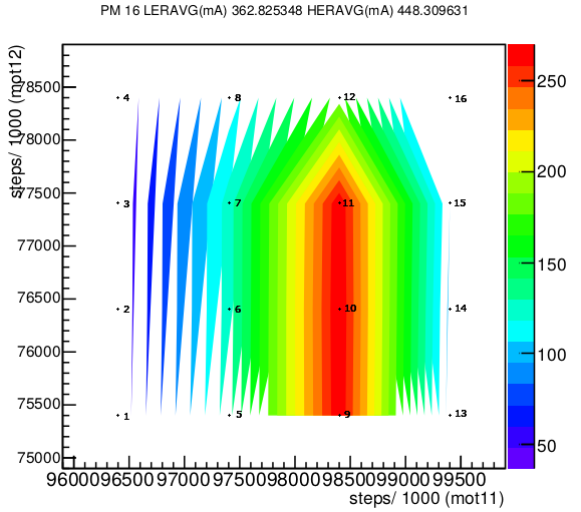

Figure 5.5: 4x4 Wide scan points, NIKKO down telescope.

The much wider NIKKO UP spot is entirely due to not having a collimator. The NIKKO DOWN feature is much weaker (a factor of 20 less counts) and thinner than that of the telescopes.

When plotting the quadratic across the points, NIKKO UP shows a robust but noisy signal over a wide number of points, consistent with expectations, Figs.5.6 and 5.7. Our Optics Box optics is not designed to handle a 20 mm beam, and changes in light acceptance across the spot are to be expected when such a wide beam enters the Box. There

is no reason to doubt that NIKKO UP will behave like OHO UP once it is properly collimated.

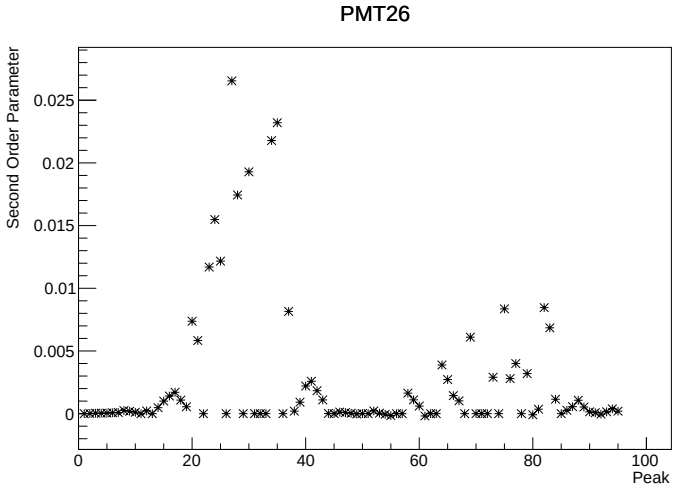

Figure 5.6: NIKKO UP telescope distribution of σ parameters for red y-polarized PMT.

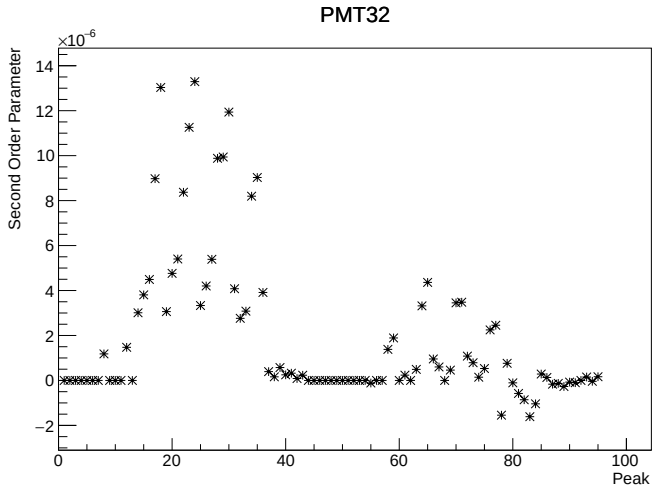

Figure 5.7: NIKKO UP telescope distribution of σ parameters for red x-polarized PMT.

Finally, NIKKO DOWN showed no signal whatsoever. The feature seen is interpreted as a reflection strip but the IP is not seen. The plan was to enter the IR in late September 2020 to examine this telescope. Coronavirus travel restrictions impeded that. We should have access during the period Dec. 20-Dec. 31 2020. This telescope has worked well in the past (as seen in the very accurate 2016 scan shown in Chapter 4). There could be mechanical problems, such as the primary mirror touching a wall and being unable to scan the whole angle inside the BP. Both OHO DOWN and NIKKO UP had similar

problems that were found and fixed in late 2019.

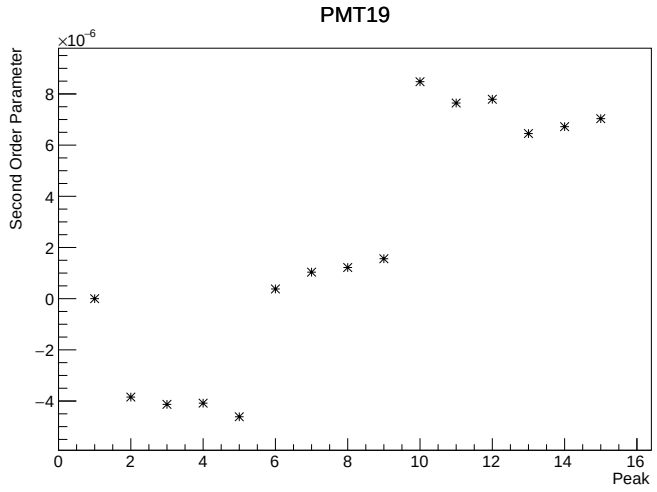

Figure 5.8: NIKKO DOWN telescope distribution of σ parameters for red y-polarized PMT.

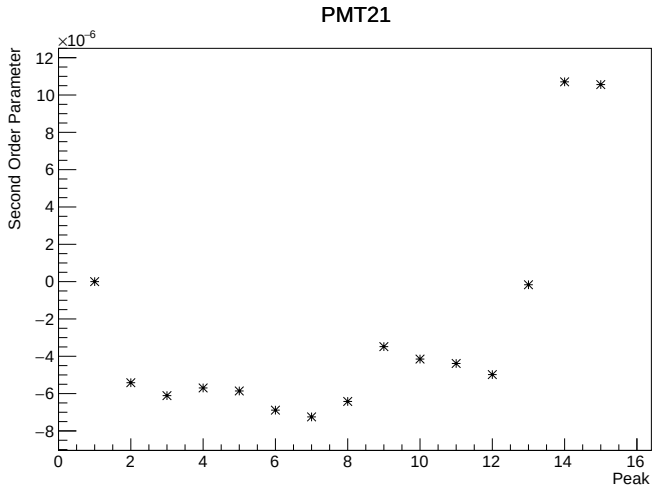

Figure 5.9: NIKKO DOWN telescope distribution of σ parameters for red x-polarized PMT.

5.5 Conclusions.

Although we are seeing clear signals after many struggles with our optics, the plan is to have all four telescopes working this Fall, or at least 3 since NIKKO DOWN may require an extended access. By working I mean the IP found by a small scan, and continuous data taking there.

We definitely need all four telescopes working in 2021. For one year we ought to run with 3 point scans (beamstrahlung spot and two adjacent points), while we continue to

develop software packages, for example making a small scan every day at midnight to measure the long term-stability of our optics. Another interesting application is to make 10 second runs at a much faster data rate (it is currently 1Hz, we would make 1kHz) to study Fourier effects on the beam-beam overlap.

As soon as we obtain a long access, perhaps in Summer 2021 but probably later, we intend to change the inside of the Optics Boxes and the front end electronics.

In the Optics Boxes we will replace the ruled gratings, which are all different, and wildly varying in efficiency as a function of wavelength (in 2014 a calibration with five different lasers was attempted with no success). They will be replaced with regular prisms, which are highly predictable in transmission rates, but make much narrower rainbows. So we will need to replace the current 28 mm PMTs with 10 mm PMTs. This replacement is also dictated by the fact that the current PMTs have pulse widths of 30 nsec or so, and the dead time due to them is starting to be an issue as the rates increase. The dead time of the smaller PMTs should be a factor of 3 less. There will be also more PMTs (from 32 to 56), so that spectral effects can be studied better.

The new electronics (being prepared at Sinaloa) will be much faster, with a resolution time of 5 nsec and a time stamp, enabling bunch-to-bunch studies. This should be the last upgrade of the LABM, and my main contribution to the project was the vast improvement in primary mirror mechanics which is allowing the much better measurements that we do today.

BIBLIOGRAPHY

[1] N. Svartholm A. Salam. *Elementary Particle Theory Stockholmm: Almguist and Wiksell*. 1968.

[2] The ATLAS Collaboration. "Observation of a New Particle in the Search for the Standard Model Higgs Boson with the ATLAS Detector at the LHC". In: *Physics Letters B* (2012).

[3] LIGO Scientific Collaboration and Virgo Collaboration. "Observation of Gravitational Waves from a Binary Black Hole Merger". In: *Phys. Rev. Lett. 116, 061102* (2016).

[4] Clement Ng. "Simulation Study of Beam-Induced Background at the SuperKEKB Interaction Region". In: *Department of Physics, The University of Tokyo* ().

[5] A. Abashian. "Belle". In: *Nucl. Instrum. Meth. A479, 117, 10.1016/S0168* (2002).

[6] H. Pollock F. Elder R. Langmuir. "Radiation from Electrons in a Synchrotron". In: *Physical Review. American Physical Society (APS)* (1947), pp. 829–830.

[7] Daniel V. Schroeder. "A posible design of large angle beamstrahlung detector". In: *doi:10.2172/6078574. URL https://www.osti.gov/servlets/ purl/6078574* (1990).

[8] J. Welch G. Bonvicini. In: *Nucl. Instrum. Meth. A418, 223* (1998).

[9] S. Di Carlo. "Ultrafast Large Angle Beamstrahlung Monitor". In: *Nucl. Instr. Meth. Phys. Res.* (2017).

[10] G. Bonvicini. *Large Angle Beamstrahlung Monitor as a Beam-Beam Monitoring Tool*. 1998.

[11] D. Cinabro G. Bonvicini and E. Luckwald. *Measurement of Colliding Beam Parameters With Wide Angle beamstrahlung*. 1999.

[12] J. D. Jackson. *Classical Electrodynamics*. 1998.

ABSTRACT

DATA ANALYSIS OF LARGE ANGLEBEAMSTRAHLUNG MONITOR

by

SAMUEL DOEG IZAGUIRRE GAMEZ

December 2020

Advisor: Prof. Giovanni Bonvicini

Major: Physics

Degree: Doctor of Philosophy

The first experimental evidence of large angle beamstrahlung at SuperKEKB is discussed in this Thesis. Beamstrahlung is the tn radiation emitted by particles belonging to one beam when they are accelerated transversely by the electro-magnetic field of the other beam. The properties of the radiation are related to the beam interaction topology and can be used to optimize the beam-beam collision. This, in turn, makes the machine's luminosity, and therefore the number of produced events, higher.

A device entirely built at WSU, the Large Angle Beamstrahlung Monitor, or LABM, has been deployed in the SuperKEKB accelerator since 2015. A five Institutions collaboration (other members have built the electronics, Data Acquisition, and Beam Pipe fittings) operates it continuously. In this Thesis the device and its operation are described in detail.

The observation of large angle beamstrahlung was made possible by a series of data analysis advances, which will ensure continuous data taking for beam monitoring as early as the Fall Run 2020.

Keywords : Beamstrahlung, Radiation, Superkekb, Japan

AUTOBIOGRAPHICAL STATEMENT

Name:

Samuel Doeg Izaguirre Gamez.

Education:

B.S. Physics, Universidad Autonoma de Sinaloa. Culiacan, Sinaloa, Mexico, 2016.

M.S. Physics, Wayne State University, Detroit, USA, 2019.

Professional Experience:

Graduate Teaching and Research Assistant, Dept. of Physics and Astronomy, Wayne State University, 2016-2020.

Biography:

I was born in Sinaloa on 1993. When I was studying high school on Mexico I interested on Physics, my mathematics teacher invited me to participate on multiple contest about physics and mathematics. After those contests I decided to study physics and earn a PhD. Those contest took me to travel around the world, I went to Paraguay, Chile, Colombia, Spain, Germany and Japan. I got married on 2017 with Fernanda, she left Mexico to joint me on Detroit and be my travel partner.